

1 *Composition and provenance of the Macigno Formation (Late Oligocene-Early Miocene) in the*
2 *Trasimeno Lake area (northern Apennines)*

3 Ugo Amendola^{1,2}, Francesco Perri², Paolo Monaco¹, Salvatore Critelli², Simonetta Cirilli¹, Tiziana Trecci¹
4 and Roberto Rettori¹

5
6 1 - Dipartimento di Fisica e Geologia, Università di Perugia, Piazza Università, 1, 06123 Perugia,
7 Italy (ugoamendola@gmail.com)

8 2 - Dipartimento di Biologia, Ecologia e Scienze della Terra, Università della Calabria, via Ponte
9 Bucci, 87036, Arcavacata di Rende (CS), Italy

10
11 **Abstract**

12 Sandstone petrography and mudstone mineralogy and geochemistry of the Late Oligocene-Early
13 Miocene terrigenous deposits of the Macigno Fm. of the Trasimeno Lake area (Central Italy)
14 provide new information on provenance, paleoenvironment, palaeoclimate, and geodynamics during
15 the early stages of the northern Apennines foreland basin setting. Sandstones are rich in trace fossils
16 and are quartzofeldspatic with various crystalline phaneritic (mostly granitoids) and medium-low
17 grade metamorphic rock fragments. Volcanic and sedimentary lithic fragments are rare.

18 The mudstone mineralogy contains a large amount of phyllosilicates, quartz, and feldspars and
19 small amount of calcite, which increases in the mid-part of succession.

20 Palaeoweathering indices (Chemical Index of Alteration with and without CaO value; CIA and
21 CIA' respectively) suggest a source area that experienced low to moderate weathering and low
22 recycling processes (on average, CIA=66.4 and CIA'=69.7). Furthermore, very low and
23 homogeneous values of Rb/K ratios (<0.006) suggest weak to moderate weathering conditions.

24 The sandstone and mudstone composition reflects a provenance derived from uplifted crystalline
25 rocks. The different amount in feldspars, the variety of lithic fragments, the occurrence of mafic and
26 carbonate input, coupled with evidence of multi-directional flows, suggest a provenance from
27 different source areas. The geochemical proxies indicate a provenance from both felsic and mafic
28 sources, predominantly for the Maestà section that shows Cr/V values ranging from 1.15 to 3.36
29 typical of source areas composed of both felsic and mafic rocks. The Western-Central Alps are
30 inferred to be the main source area of the Macigno foreland system, but signals from the
31 Mesomediterranean Microplate have also been suggested. These new data suggest that the Macigno
32 Fm. was probably located in a peculiar area which received either distal fine turbidite flows from
33 the northernmost Alpine area and residual sandy debris flows coming from the westernmost Alps.

34

35 Key words: gravity flow deposits; Northern Apennines; composition; provenance;
36 palaeoweathering; palaeoenvironment

37 1. Introduction

38 The thrust belt-foreland system of Northern Apennines was characterized by a continuous eastward
39 migration of depocentres reflecting detachment of subducted lithosphere as result of African-
40 European collision in the Late Eocene and subsequent rollback during the Late Oligocene to Recent
41 time (Van der Meulen et al., 1998; Dinelli et al., 1999; Barsella et al., 2009). During the Oligocene-
42 Miocene, foredeep depocentres were filled by thick debris of turbidite deposits in continuous and
43 complex depositional units. The Macigno Fm. represents the first depositional unit of the Late
44 Oligocene-Early Miocene foreland basin system of northern Apennines, linked to Alpine sectors
45 through longitudinal feeding of the foreland basin (Ricci Lucchi, 1986; 1990). The Macigno Fm. is
46 traditionally divided into a westernmost and oldest portion (late Chattian), cropping out along the
47 Tuscan coast and named “Macigno Costiero” and an eastern and younger portion (late Chattian-
48 Aquitanian) named “Macigno Appenninico” thrust eastward on the Marnoso-arenacea Formation in
49 the Casentino area (Boccaletti et al. 1990; Milighetti et al. 2009 among others). The Modino-
50 Cervarola-Trasimeno units and associated facies (now included in eastern Macigno) and the
51 overlying Marnoso-Arenacea Fm. represent the Mid-Late Miocene foreland basin system, whereas,
52 the depositional framework and basin architecture of the foreland system are well developed (Ricci
53 Lucchi, 1986; 1990; Centamore et al. 2002; Guerrera et al., 2012). Differently to Ricci Lucchi
54 (1986. 1990), Valloni et alii (1991), Pandeli et alii (1994) and recently Barsella et alii (2009)
55 indicated only one terrigenous source area for the Macigno Fm., identified with the western-central
56 Alps. Other authors recently claim that alpine source interfingered with an increasing contribution
57 from the emerging Apennines from the Early Miocene onward, involving the upper portion of the
58 Macigno Formation, especially the Modino-Cervarola unit (Gandolfi et al., 1983; Andreozzi and Di
59 Giulio, 1994; Di Giulio, 1999). According to Cornamusini (2002) and Cornamusini et alii (2002),
60 new sedimentological and petrographic data suggest that the Corsica-Sardinian Hercynian basement
61 is the source area of the debris flow and turbidite sandstones of the “Macigno Costiero”. Thus, the

62 hypothesis indicating a multi-source area for the Macigno Fm. can be strongly considered. Changes
63 in sandstone composition of perisutural basins usually reflect complex provenance relationships
64 from local to distal source areas, where long-distance transport is generally associated with
65 Apenninic longitudinal orientation of flows. The local derivation of terrigenous, coarse grained and
66 massive material is generally transverse from the west (e.g. Zuffa, 1987; Critelli et al., 1990;
67 Critelli, 1993). This mixed provenance is typical of remnant ocean basin-fill (Critelli et al., 1990;
68 Critelli, 1993) and foreland basin systems (Zuffa, 1987; Critelli, 1999; Critelli et al., 2007).

69 The aim of this work is to use a multi-disciplinary approach to provide useful information on the
70 provenance of the Macigno Fm. sandstones for unraveling both local and distal terrigenous
71 dispersal. For this purpose a detailed study of the Late Oligocene-Early Miocene sandstones and
72 mudstones characterizing the Macigno Fm. of the Trasimeno Lake area, previously analyzed by
73 sedimentological and ichnological point of view (Monaco and Trecci, 2014), has been done. The
74 petrographical, mineralogical, and geochemical proxies are aimed to better understand the
75 composition, provenance, and paleoclimatic signatures during the development of a foredeep basin
76 system. Petrographic study of the coarse-grained fraction coupled with chemical and mineralogical
77 analyses of the fine-grained fraction represents a thorough tool to investigate the processes that
78 occurred from sediment generation on the exhumed uplands to the final deposition on foredeep
79 basins. Detrital modes of sand reflect the cumulative effects of source rock composition, chemical
80 weathering, hydraulic sorting, and abrasion (Suttner, 1974; Basu, 1985; Johnsson, 1993; Nesbitt et
81 al., 1996).

82 The distribution of major and trace elements related to the mineralogical composition of fine-
83 grained sediments is an important factor to reconstruct the source-area composition, the weathering
84 and the diagenetic processes (e.g. Condie et al., 1992, 2001; Bauluz et al., 2000; Mongelli et al.,
85 2006; Critelli et al., 2008; Zaghloul et al., 2010; Caracciolo et al., 2011; Perri, 2014; Perri and Ohta,
86 2014).

87 The X-ray diffraction (XRD) and X-ray fluorescence spectrometry (XRF) have been used to study
88 and characterize the mineralogical and chemical variations of the mudstone samples, whereas the
89 sand fraction has been studied by petrographic analysis. By combining the information deduced
90 from these analyses, it is possible to outline possible variations on source areas and, thus, to explain
91 and predict the sedimentary evolution and geological processes affecting the studied sediments.

92 Moreover the relationship developed between source area and sedimentary basin can be also
93 defined.

94

95 **2. Geological setting**

96 The Northern Apennines are basically composed of two tectonic complexes: (1) the remnants of a
97 Cretaceous–Paleogene accretionary wedge (Ligurian Complex), generated by the Africa–Europe
98 convergence, thrust on top by (2) an Oligocene–Miocene terrigenous complex (Ricci Lucchi, 1986)
99 that was accreted in a retreating subduction zone overriding the Adriatic continental margin (e.g.,
100 Castellarin 1992). This second terrigenous complex is composed of different units: the Macigno and
101 Modino turbiditic units of late Chattian to early Aquitanian age (25–23 Ma), the Monte Cervarola
102 Fm. of late Aquitanian to early Langhian age (21–16 Ma), and the Marnoso-arenacea Fm. of
103 Langhian to Tortonian age (14–9 Ma) (Guerrera et al., 2012) (Fig. 1). The Late Oligocene–Early
104 Miocene Macigno foredeep system was a basin 250–300 km in length, almost 50 km in width, and
105 NW–SE oriented, starting from the modern Emilia (Northern Italy) to the Latium–Umbria border
106 (Hill and Hayward, 1988; Boccaletti et al., 1990). The studied sections outcropping at the north of
107 Trasimeno Lake (Fig. 2) belong to a N–S elongated Macigno Fm. basin deposited in the Tuscan
108 Domain that were overthrust eastwards over the innermost sedimentary successions of the Umbria
109 Domain (Canuti et al., 1965).

110 In the northern area of the Trasimeno Lake, the Macigno Fm. overlies the Scaglia Toscana Fm.
111 (Cretaceous - Late Eocene) (Piccioni and Monaco 1999; Plesi et al., 2002). The Scaglia Toscana

112 **Fm.** (about 200 m thick) is made of limestones, marly limestones, variegated marls and dark pelitic
113 beds with many coarse- to very fine-grained grained turbidites (Damiani et al., 1987; Ielpi &
114 Cornamusini 2013; Monaco et al. 2012). The Middle-Late Eocene portion is characterized by mud
115 turbidites containing a typical deep-sea Nereites ichnofacies, with an ichnocoenosis at *Avetoichnus*
116 *luisae*, *Chondrites intricatus*, *C. targionii*, *Cladichnus*, *Taenidium* and *Ophiomorpha rudis* (Monaco
117 et al., 2012). These deposits show an increasing upwards contribution of clayey-marly and clayey
118 lithotypes, respectively (Piccioni and Monaco, 1999; Monaco and Uchman, 1999; Monaco et al.,
119 2012).

120 The Macigno Fm. is subdivided into three members: the Molin Nuovo Member (MAC1), the
121 Poggio Belvedere Member (MAC2), studied in detail in this work, and the Lippiano Member
122 (MAC3) (see detailed description in Trecci and Monaco, 2011). The lower portion of the Macigno
123 Fm. (500-600 m of maximum thickness), the Molin Nuovo Member, consists of thick-bedded
124 facies, gradually replaced upward by a thinner facies. Facies assemblages indicate various deposits
125 (in lithology and thickness), often arranged in thickening-upward sequences that can be related to
126 depositional lobes of deep-sea fan (*sensu* Einsele, 1991). Thickening upward sequences are present
127 even in the basal part of the Poggio Belvedere Member, while stationary sequences are common in
128 the middle-upper portion of the Lippiano Member. Thick-bedded sandstones of outer lobes are
129 interposed with thin-bedded, arenaceous pelitic and calcareous turbidites and lobe-fringe deposits of
130 basin plain dominated by thin-bedded and fine-grained facies. The maximum thickness of the
131 Poggio Belvedere Member is about 300 m, and its age has been attributed to the Chattian (MNP25b
132 subzone, see Plesi et al., 2002 for the micropaleontological content). The lower units contain
133 slurred beds (Ricci Lucchi and Valmori, 1980) and calcareous levels (“*areniti ibride*”, Zuffa, 1980
134 or “*torbiditi calcaree*”, Bruni and Pandeli, 1980; Pietralavata Bed, Plesi et alii, 2002; Brozzetti,
135 2007). These carbonatic deposits, outcropping in the northern sector about 40 m above the bottom
136 of Poggio Belvedere Member, are the most important calcareous beds for thickness and lateral

137 continuity. Probably they can be correlated with the “Polvano Bed” described by Aruta et al. (1998)
138 for the Cortona area (Brozzetti, 2007). Nannofossil assemblages (Plesi et al., 2002) point to the Late
139 Chattian-Early Aquitanian age (MNP25b-MNN1b) for the Poggio Belvedere Member. In the
140 overlying Lippiano Member, the thinner facies, tabular beds (with flat basal surfaces and good
141 lateral continuity, *sensu* Einsele, 1991) are dominant, typically of distal, basin plain environment.
142 The calcareous beds are more frequent than in the Poggio Belvedere Member (Aruta, 1994; Aruta
143 and Pandeli, 1995; Aruta et al., 1998). Biostratigraphic investigation (Plesi et al., 2002) suggests a
144 Late Aquitanian age (MNP25b-MNN1b) for the Lippiano Member. In the overall Macigno Fm.
145 multidirectional grooves and flute casts indicate mainly NW/SE oriented paleocurrents, with a SE
146 preferential flow direction, and minor W oriented flows (e.g. slurried beds and slumps) (see in detail
147 below). The direction of carbonate turbidites remains controversial and needs further investigations.

148

149 **3. Stratigraphy, facies and ichnocoenoses of the studied sections**

150 Three stratigraphic sections belonging to Poggio Belvedere Mb. (MAC2) have been studied in the
151 Trasimeno Lake area (Fig. 2), and were sampled for the purposes of the present study. The studied
152 sections were sampled near Cortona along the SP35 road from Cortona (Tuscany) to Umbertide
153 (Umbria) in three distinctive areas where are in stratigraphical continuity: the Pianello, Renali and
154 Maestà Stratigraphic sections (Fig. 3).

155

156 *3.1 Pianello Stratigraphic section*

157 The section (Fig. 4A-B-C) is more than 25 m thick and rests on Early Oligocene Molin Nuovo Mb.
158 (MAC1). The Pianello section is characterized by a diverse facies assemblage that includes massive
159 to laminated thin-bedded coarse-grained sandstones (F5-F6-F7 facies of Mutti, 1992), up to 2-4 m
160 thick, 0.5 m thick slurried beds (F1-F2 facies of Mutti, 1992) and alternance of hemipelagic

161 mudstones and fine-grained turbidites (F8-F9a-b facies of Mutti, 1992) which are frequently
162 bioturbated.

163 The sandy horizons have been interpreted as transitional high-density turbidites (Mutti, 1992) or
164 cohesive sandy debris flow deposits (Shanmugan, 2002). They partially include pebbles, mud lumps
165 and several vegetal fragments and decrease in thickness going toward the mid-upper portion of the
166 section in which the mudstones and mud turbidites begin to prevail. Fine-grained turbidites contain
167 plane-parallel and convolute laminae and are associated to the T_{b-e} Bouma facies. These levels
168 include a rich ichnocoenosis, typical of basin plain depositional area of the *Nereites* ichnofacies,
169 mainly represented by hypichnial to epichnial and exichnial trace fossils (Monaco and Trecci,
170 2014). The abundant trace fossils are *Halopoa imbricate*, *Phycosiphon* sp., *Spirophycus bicornis*.
171 The common trace fossils are *Chondrites intricatus*, *Ophiomorpha rudis*, *Ophiomorpha annulata*,
172 *Trichichnus* sp., *Spirorhapse involuta*, whereas *Palaeophycus tubularis* is rare.

173 Slurried beds are easily recognizable for the inner subdivision of the beds in three intervals: a)
174 coarse-grained basal sandstone interval, b) an intermediate swirly appearance (*sensu* Ricci Lucchi
175 and Valmori, 1980) and, on the top, c) a fine-grained sandstone interval referred as F9a (Trecci and
176 Monaco, 2011 and references therein). Slurried beds occur through the entire stratigraphical section
177 and they are often intercalated with fine-grained turbidites. They come from a close slope area and
178 probably are derived from co-genetic debrite-turbidite composite flows (Ricci Lucchi and Valmori,
179 1980; Talling et al., 2004; see types of Muzzi Magalhaes and Tinterri, 2010).

180 Palaeocurrent data show predominant NW-oriented flows for fine-grained turbidites and some
181 massive sandy horizons. However several groove casts, individuated in the uppermost facies of the
182 coarse-grained sandstones and slurried divisions, clearly indicate W-oriented flows (Fig. 4B). Thus
183 two types of groove casts have been recovered with an angle from 20 to 40 °. The facies assemblage
184 of Pianello Stratigraphic section reflects a transition from outer lobe, indicated by coarse-grained

185 sandstone horizons, to fringe-basin plain facies, represented by fine-grained turbidites, and outlines
186 a slight deepening of the depositional system.

187

188 3.2 Renali Stratigraphic section

189 The section (Fig.4D) is more than 20 m thick and overlies deposits of the Pianello section. The
190 section is characterized by an increase of rhythmical fine-grained turbidites (F9a-b facies).
191 Laminated beds (T_b of Bouma facies) are thicker than the convolute laminae interval (T_c of Bouma
192 facies) and they can reach 1 m in thickness.

193 Ichnocoenosis is quite similar to that analyzed in the previous section. Differences consist of larger
194 amounts of *Ophiomorpha annulata*, *Halopoa*, *Phycosiphon*, *Planolites* and *Spirorhapse*. Similarly
195 to previous section *Spirophycus bicornis* is abundant whereas *Paleodictyon maximum* and *P.*
196 *strozzii* are common. Also *Helmintorhapse* sp. and *Cosmorhapse lobata* occur (Fig. 5A-B)
197 (Monaco and Trecci, 2014). Coarse-grained sandstone facies (F5-F6-F7 facies), up to 2 m thick,
198 only appear in the basal and upper portion, and they are totally absent in the central part where fine-
199 grained turbidites are dominant. Slurried beds, up to 1.5 m thick, show similar characteristics to
200 those described for the previous section but they are less frequent. Moreover, in the basal portion of
201 analyzed section, laminated to convoluted calciturbidite deposits, up 2-3 m thick, occur (Fig. 4D).
202 They are well sorted, and have sharp basal contacts and tabular top surfaces and that include graded
203 and laminated to convoluted Bouma T_{a-e} facies (Trincardi et al., 2005; Shanmughan, 2006; Monaco
204 et al., 2009; Trecci and Monaco, 2011).

205 Paleocurrent data show a NW-oriented flow for fine-grained turbidite facies. As seen in the
206 previous section, multi-directional flows have been observed. In some thin laminated beds (F9b
207 facies) flute casts clearly indicate W-oriented turbidite flows although groove casts individuated in
208 calciturbidite levels show paleoflows towards the S and SW. The facies assemblage of Renali area

209 thus reflects a basin plain environment, which locally received gravity flows coming from a very
210 close slope area.

211

212 3.3 Maestà Stratigraphic section

213 The section (Fig. 4E-F) is more than 20 m thick and overlies deposits of Renali section and is
214 overlain by Early Miocene Lippiano Mb. (MAC3). The section consists of mostly rhythmical, fine-
215 grained turbidites (F9a-b facies) up to 5-6 m thick, which are interfingered by thin slurried beds, up
216 0.5 m thick and thin-bedded coarse-grained sandstones (F4-F7-F8 facies of Mutti 1992), up 0.5-0.7
217 m thick. Laminated and convoluted facies (F9a-b facies of the same Author, Fig. 4F) are thinner
218 than the Renali section, and the mudstone intervals are more abundant. The ichnocoenosis is
219 dominated by an abundant endichnial/hypichnial *Halopoa* (both *H. embricata* and *H. var.*
220 *fucusopsis*), which occur in conspicuous amount in every thin beds, with *Spirorhapse involuta* and
221 *Urohelminthoida dertonensis*. *Chondrites*, *Paleophycus*, *Planolites*, *Ophiomorpha* and *Trichichnus*
222 are rarer than in previous sections. Of particular significance is the occurrence of large *Spirophycus*
223 *bicornis* with abundant *Spirorhapse involuta*, *Paleodictyon minimum*. Also *P. strozzii* and
224 *Urohelminthoida dertonensis* occur (Fig. 5C-D-E-F) (Monaco and Trecci, 2014).

225 Paleocurrent data only show NW-oriented flows. The Maestà section facies indicate a deeper basin
226 plain environment, locally with turbidites and other residual gravity flows coming from a slope area
227 that was probably rarer than the depositional system depicted for Renali area.

228

229 4. Sampling and analytical methods

230 Sandstones and mudstones were sampled along the Poggio Belvedere Mb. (MAC2) in the Cortona
231 area (Figures 2 and 3). The sampling was concentrated in those parts of the succession, which are
232 better exposed and preserved and thicker than in other analogue area of Trasimeno Lake. For the

233 purpose of this study, we selected and analyzed only sandstone strata. Some strata show abundant
234 carbonate particles (Renali area) characterized by carbonate clasts and fossils in both graded and
235 laminated turbidite facies. These samples were only qualitatively described and not included in the
236 recalculated analysis of the sandstones.

237 Nineteen medium-to coarse-grained sandstone samples were selected for thin-section preparation
238 and modal analysis. Thin sections were etched with HF and stained by immersion in sodium
239 cobaltonitrite solution to allow the identification of feldspars. More than 400 points were counted
240 through the use of a petrographic microscope in each thin section according to the Gazzi-Dickinson
241 method (Gazzi, 1966; Dickinson, 1970; Ingersoll et al., 1984; Zuffa, 1985). Recalculated grain
242 parameters are defined according to Dickinson (1970), Ingersoll and Suczek (1979), Zuffa (1985),
243 Critelli and Le Pera (1994, 1995), and Critelli and Ingersoll (1995).

244 Mudstone samples were crushed and milled in an agate mill to a very fine powder. The powder was
245 placed in an ultrasonic bath at low power for a few minutes for disaggregation.

246 The mineralogy of the whole-rock powder was obtained by X-ray diffraction (XRD) using a Bruker
247 D8 Advance diffractometer (CuK α radiation, graphite secondary monochromator, sample spinner;
248 step size 0.02; speed 1 sec for step) at the University of Calabria (Italy). Semiquantitative
249 mineralogical analysis of the bulk rock was carried out on random powders measuring peak areas
250 using the WINFIT computer program (Krumm, 1996). The strongest reflection of each mineral was
251 considered, except for quartz for which the line at 4.26 Å was used instead of the peak at 3.34 Å
252 because of its superimposition with 10 Å-minerals and I-S mixed layer series. The abundance of
253 phyllosilicates was estimated measuring the 4.5 Å peak area. The percentage of phyllosilicates in
254 the bulk rock was split on the diffraction profile of the random powder, according to the following
255 peak areas: 10–15 Å (illite–smectite mixed layers), 10 Å (illite+micas), and 7 Å (kaolinite+chlorite)
256 minerals (e.g. Cavalcante et al., 2007; Perri, 2008).

257 Whole-rock samples were prepared by milling to a fine powder in an agate mill. Elemental analyses
258 for major and some trace elements (Nb, Zr, Y, Sr, Rb, Ba, Ni, Co, Cr, and V) were obtained by X-
259 ray fluorescence spectrometry (XRF) using a Bruker S8 Tiger equipment at the University of
260 Calabria (Italy), on pressed powder disks of whole-rock samples. These data were compared to
261 international standard-rock analyses of the United States Geological Survey (e.g., Flanagan, 1976).
262 The estimated precision and accuracy for trace element determinations are better than 5%, except
263 for those elements having a concentration of 10 ppm or less (10–15%). Total loss on ignition
264 (L.O.I.) was determined after heating the samples for 3 h at 900 °C.

265

266 5. Sandstone petrology and detrital modes

267 Samples include massive coarse-grained sandstones from the lobe-fringe facies (from F5 to F7
268 facies; Mutti, 1992), slurried divisions (F2 facies; related to residual dense flows), related to
269 residual dense flows, and graded-laminated sandstones from rhythmical fine turbidites (F8-F9a-b
270 facies; related to low-density flows), related to low-density flows. The studied quartzofeldspathic
271 sandstones are composed of moderately to poorly sorted, siliciclastic grains.

272 Raw point-count data of sandstones are in Table 1, whereas the recalculated modal point-count data
273 are in Table 2.

274 a) Pianello Stratigraphic Section

275 Sandstones of the Pianello area range from massive sandstones of an outer lobe facies (P1, P23, P3,
276 P5 samples) to fringe deposits of a basin plain (P2, P21, P22, P18 samples) with a single sample
277 from a slurried division (P26 sample). The quartzofeldspathic sandstones have an average
278 composition of $Q_{m48}F_{40}L_{t12}$ (Fig. 6), and the Qm/F (Quartz monocrystalline/Feldspars) ratio is
279 1.33. These sandstones have variable sedimentary versus metasedimentary lithic fragments (average
280 value: $L_{m86}L_{v1}L_{s13}$; outer lobe facies: $L_{m83}L_{v3}L_{s34}$; fringe-basin plain: $L_{m88}L_{v0}L_{s12}$; slurried

281 division: $Lm_{89}Lv_0Ls_{11}$; Fig. 6; Tab. 2). Feldspars (both plagioclase and K-feldspars) are the most
282 abundant constituents in the lobe-fringe facies ($Qm_{39}F_{46}Lt_{15}$; $Qm/F= 0.94$). In particular feldspar
283 content reaches the highest content in W-oriented grain flow deposits of the lobe facies (i.e. P5=
284 $Qm_{36}F_{49}Lt_{15}$; $Qm/F= 0.73$) of the mid-upper portions of the stratigraphic section. Plagioclase is
285 dominant (average $P/F=0.66$), and fresh grains are slightly more abundant than altered ones. Some
286 plagioclase crystals display albite polysynthetic twinning (Fig. 7A). Quartz grains are also
287 abundant, mainly as monocrystalline subrounded to angular and subspherical grains. Quartz grains
288 are more prevalent in fringe-basin plain facies ($Qm_{55}F_{34}Lt_{11}$; $Qm/F= 1.65$) and slurried divisions
289 ($Qm_{56}F_{39}Lt_5$; $Qm/F= 1.44$) than in the external lobe sandstones. Polycrystalline grains also occur in
290 large amounts ($Qp_{73}Lvm_1Lsm_{26}$) and have similar tectonics-fabric versus plutonic-fabric. Dense
291 minerals include garnet, epidote and zircon. Metasedimentary lithic grains are not abundant and
292 they include phyllite, slate and fine-grained micaschist (Fig. 7B). Sedimentary rock fragments occur
293 in discrete amounts in the outer lobe facies (i.e. P23 sample). A few volcanic lithic grains are also
294 present (P23 sample) and they exhibit a felsic granular texture with plagioclase and minor quartz
295 phenocrysts (Fig. 7C). Abundant phaneritic fragments of plutonic rocks, mostly plagioclase-rich
296 granodiorite and tonalite, with minor granite (Fig. 7D), and coarse gneissic fragments also occur
297 (average value; $Rg_{70}Rs_3Rm_{27}$; outer lobe facies: $Rg_{66}Rs_5Rm_{29}$; distal turbidite facies: $Rg_{73}Rs_2Rm_{25}$;
298 slurried division: $Rg_{73}Rs_3Rm_{24}$). In the outer lobe facies samples, several high-medium grade
299 metamorphic (Fig. 7E) and some sedimentary fragments occur.

300 Lithic fragments, especially felsic volcanic fragments, in sandstone modes of the Pianello area are
301 less abundant than those from the Macigno Fm. (Fig. 8; Tab. 3). In detail, sandstones of outer lobe
302 facies are more feldspar-rich than both “Macigno Appenninico” of Northern Tuscany (Di Giulio,
303 1999: $Qm_{59}F_{29}Lt_{17}$; Bruni et al., 2007: average value, $Qm_{50}F_{34}Lt_{16}$) and the “Macigno Costiero” of
304 Southern Tuscany (Cornamusini, 2002: $Qm_{57}F_{19}Lt_{24}$). Also Poggio Belvedere sandstones of this
305 study are more felsic enriched than those analyzed by Barsella et al., 2009 ($Qm_{36-61}F_{14-24}Lt_{10-25}$; Fig.

306 8). However, Plesi et alii (2002) report a similar feldspar-rich trend in the lower sandstones of
307 Poggio Belvedere Mb. collected in the High Tiber valley (Umbria). Likely, Bruni et alii (2007)
308 point out a slight feldspar enrichment at the transition of the Lower-Upper Macigno Fm. in Abetone
309 area (NW Tuscany) (max F=35.6%, Qm₄₄F₄₄Lt₁₂; see GO 24 sample in Fig. 8). Differently,
310 sandstones of basin plain facies have a composition that can be comparable with the average value
311 indicated for Macigno Fm. (Valloni et al., 1991; Di Giulio, 1999; Bruni et al., 2007; Barsella et al.,
312 2009) (Tab. 3).

313 *b) Renali Stratigraphic Section*

314 Sandstones collected along the Renali stratigraphic section are in outer lobe-fringe facies (R7 and
315 R3 samples), basin plain facies (R12 and R5 samples) and slurred divisions (R10 and R15
316 samples). Other samples were collected in the calcareous turbidite facies (R1, R2 and R9 samples)
317 but they were not counted with the Gazzi-Dickinson method so they are only qualitatively
318 described. The sandstone composition is quartzofeldspathic (average value: Qm₅₉F₃₀Lt₁₂; outer
319 lobe-fringe facies: Qm₆₁F₃₀Lt₉; basin plain facies: Qm₅₆F₃₂Lt₁₂; slurred division: Qm₆₀F₂₇Lt₁₃). The
320 average Qm/F ratio is 1.93.

321 These sandstones have similar amounts of sedimentary versus metasedimentary lithic fragments
322 (average value: Lm₆₃Lv₁₁Ls₂₆; outer lobe facies: Lm₆₉Lv₁₉Ls₁₂; basin plain facies: Lm₆₁Lv₁₃Ls₂₆;
323 slurred division: Lm₅₇Lv₁Ls₄₂; Fig. 6). Quartz grains are the most abundant constituents in all the
324 sampled facies and their amount remain almost homogeneous with a slight peak in the outer lobe
325 facies. Quartz grains show the same textural characteristics seen in the previous section, with a
326 sharp prevalence of monocrystalline grains on polycrystalline grains, more marked than in the
327 previous section (Qp₅₄Lvm₉Lsm₃₇) (Fig. 7F). Feldspars (both plagioclase and K-feldspars) are also
328 abundant and maintain a constant ratio with the quartz grains. Many feldspar grains are altered; they
329 are sericitized and partially clay altered. The plagioclase versus total feldspars ratio is higher than
330 that of the previous section (P/F=0.74). Metasedimentary lithic grains are not so abundant and they

331 include phyllite, slate and fine-grained micaschist, including also few chloriteschist fragments.
332 Siltstone and chert fragments are also present. Volcanic lithic fragments **are more abundant than in**
333 the other sections (with a prevalence in R7 sample) and **they** occur in both outer lobe and distal
334 turbidites facies (Fig. 7G). Abundant phaneritic fragments of plutonic rocks, mostly plagioclase-rich
335 granodiorite and tonalite, with minor granite also occur (average value $Rg_{65}Rv_3Rm_{32}$;
336 $Rg_{62}Rs_9Rm_{29}$). Coarse gneissic fragments are rare. Micas grains, including either muscovite, biotite
337 and chlorite, **are abundant**. Carbonate constituents are only present in R1, R2, **and** R9 samples,
338 collected within calciturbidite levels, and R10 sample (Fig. 7H). Biofacies related to these levels are
339 reported in detail in 5.1.

340 The interstitial component of siliciclastic arenites includes detrital fine siliciclastic matrix, and rare
341 authigenic minerals and pseudomatrix. Only in the carbonate samples the interparticle porosity is
342 partially filled by sparite and microsparite calcite cement and relatively fine carbonate matrix.

343 **Differently** to previous data of the Macigno Fm., the Renali sandstones are quite similar to those of
344 the “Macigno Appenninico” of Northern Tuscany (Di Giulio, 1999: $Qm_{59}F_{29}Lt_{17}$; Bruni et al., 2007:
345 average value, $Qm_{50}F_{34}Lt_{16}$) and the Poggio Belvedere Mb. sandstones of Trasimeno Lake area
346 (Plesi et al., 2002, $Qm_{40-55}F_{20-50}Lt_{10-25}$; Barsella et al., 2009, $Qm_{36-61}F_{14-24}Lt_{10-25}$; Tab. 3). The lithic
347 composition is quite similar to that reported by Cornamusini (2002) for the Macigno Costiero in
348 Southern Tuscany ($Lm_{66}Lv_{19}Ls_{15}$). **The** volcanic lithic percentage is similar (Renali area: $Lv=13$;
349 Macigno Costiero: $Lv>13$) although the means of volcanic index ($Iv=Lv/L\%$) is properly more
350 compatible with Macigno Fm. of Chianti Hills area (Renali: $Iv=11.25$; Macigno Costiero: $Iv=19$;
351 Macigno del Chianti: $Iv=11.5$. Data from Cornamusini, 2002; see Tab. 3 and Fig. 8).

352 c) *Maestà Stratigraphic Section*

353 Sandstones of the Maestà section are included in **the** lobe-fringe facies (M1 and M3 samples), basin
354 plain facies (M8 sample) and slurried divisions (M5 sample). Sandstones are quartzofeldspathic

355 (average value: $Qm_{64}F_{30}Lt_6$). The average Qm/F ratio is 2.52, the highest value in the Poggio
356 Belvedere Mb..

357 The overall lithic content is **less abundant than** the other sections and the metasedimentary lithic
358 fragments are always more abundant than **the** sedimentary fragments (average value: $Lm_{82}Lv_0Ls_{18}$;
359 [Fig. 6](#)). Quartz grains are the most abundant constituents in all the studied facies and their amount
360 reaches a large amount in laminated sandstones of lobe-fringe facies (F7 facies), sampled in the
361 mid-top part of the section (M3 sample: $Qm=79\%$; $Qm/F=4.77$). Quartz grains show high sorting
362 and occur as subrounded and subspherical monocrystalline grains. Feldspars (both plagioclase and
363 K-feldspars) are abundant, and plagioclase versus total feldspars ratio is high as well in Renali
364 section ($P/F=0.76$). The few metasedimentary lithic grains include fine-grained micaschist,
365 comprising also few chloriteschist fragments, and rare slate and phyllite. Siltstone fragments are
366 rare or absent, whereas chert grains are present (e.g. M1 sample; F4 facies). Phaneritic fragments of
367 plutonic rocks occur, and metamorphic fragments result to prevail in some laminate sandstones
368 (average value $Rg_{43}Rs_{10}Rm_{47}$). Coarse gneissic fragments are rare.

369 Similarly to Renali area, the Maestà sandstones can be compared to both Macigno Appenninico of
370 Northern Tuscany ([Di Giulio, 1999](#): $Qm_{59}F_{29}Lt_{17}$; [Bruni et al., 2007](#): average value, $Qm_{50}F_{34}Lt_{16}$)
371 and Poggio Belvedere sandstones of Trasimeno Lake ([Barsella et al., 2009](#): $Qm_{36-61}F_{14-24}Lt_{10-25}$)
372 ([Fig. 7](#)), although average feldspar is considerably higher, and lithic composition is subordinate.
373 The lithic percentage is quite similar to that reported by [Cornamusini \(2002\)](#) for the Macigno del
374 Chianti in Southern Tuscany ($Lm_{82}Lv_{11}Ls_7$), with differences in volcanic amount. These sandstones
375 show some similar petrological characteristics with Renali sandstones excepting for average lithic
376 component and missing of volcanic grains.

377

378 *5.1 Biotic assemblage of calciturbites*

379 The samples collected in graded-laminated intervals of calciturbidites (R1 sample: F8 facies)
380 (*rudstone* texture; Dunham, 1962; Embry and Klovan, 1971) comprise several mm to cm-sized
381 **?Eocene to ?Early Miocene** macroforaminifers, including mainly alveolinids, nummulitids and
382 lepidocyclinids with small benthic shallow water and deep water foraminifers (Fig. 7H).
383 Extrabasinal carbonate grains are present and they include biomicritic and peloidal limestones,
384 coralline algae (*Rhodophyta*), thick shelled bivalves, echinoids and bryozoan fragments. Planktonic
385 **foraminifers** (globigerinids) and porcelaneous small **foraminifers** (miliolids), coupled with
386 radiolarians, sponge spicules and ostracods, have been recorded as mm-grained extrabasinal grains
387 in wackestones. Samples from laminated-convolute facies (R9 and R2; F9a-b) have mixed
388 carbonate-siliciclastic composition (hybrid arenites *sensu* Zuffa, 1980) with abundant skeletons of
389 bivalves and benthic foraminifers, and angular silt-size quartz and micas grains.

390

391 5.2 Comparison with modern sands of Calabria

392 Detrital modes of Macigno **Fm.**, studied here, can be compared with those of Calabrian Arc modern
393 sands reported from Ibbeken and Schleyer (1991) and Perri et alii (2012b) (Tab. 3). Valloni et alii
394 (1991) and Di Giulio (1999) **have done similar studies.**

395 In general, the average value of **the** Macigno Fm. sandstones (Qm₅₇F₃₄Lt₉; this study) is quite
396 similar to **the** average value **of** modern sands of Calabria (Qm₅₁F₂₈Lt₂₁, Ibbeken and Schleyer, 1991)
397 **except** for a visible depletion in **the** fine-grained lithic component.

398 In detail, the mean of **the** detrital modes in sandstones of **the** Pianello Stratigraphic section
399 (Qm₄₉F₄₀Lt₁₁, Qm/F= 1.33) are comparable with granite-sourced modern sands analyzed by
400 Ibbeken and Schleyer (1991) in which **the** average value is Qm₄₆F₃₃Lt₂₁ **with a** Qm/F ratio **of** 1.3
401 (see Tab. 3). In particular W-oriented sandstones of **the** outer lobe-fringe facies (Qm₃₉F₄₆Lt₁₅,
402 Qm/F= 0.94) are very similar with modern Calabrian sands of **the** Neto-Lipuda petrofacies

403 ($Qm_{36}F_{46}Lt_{18}$, $Qm/F= 0.8$; data reported from Perri et al., 2012b) deposited in the Ionian sea
404 offshore that is derived from a plutonic-dominated source area (Sila Massif).
405 Differently from Pianello stratigraphic section, detrital modes of the Renali (average value:
406 $Qm_{58}F_{31}Lt_{11}$, $Qm/F= 1.93$) and the Maestà sandstones (average value: $Qm_{64}F_{30}Lt_6$, $Qm/F= 2.52$)
407 show similar petrological characteristics with granitoid plus metamorphic-sourced modern
408 Calabrian sands ($Qm_{55}F_{24}Lt_{21}$, $Qm/F \geq 2$) reported from Ibbeken and Schleyer (1991). Thus, there is
409 a visible depletion in felsic grains going from the Pianello toward the Renali and Maestà
410 Stratigraphic sections (see section 7).

411

412 6. Mineralogical and geochemical composition of mudstones

413 6.1 Mineralogy of mudstones

414 Whole-rock XRD analyses (Table 4) indicate that phyllosilicates are the main mineralogical
415 components, ranging from 48% to 69% of the bulk rock. Illite and mica prevail with values up to
416 53%, whereas chlorite ranges from 10% to 25%. Kaolinite occurs in minor amounts. Among the
417 interstratified minerals, the I-S mixed layers are slightly more abundant, but the amounts of C-S
418 mixed layers are less abundant. The non-phyllosilicate minerals are represented by quartz, feldspars
419 (plagioclase and K-feldspar) and carbonates (calcite and dolomite). Quartz ranges from 20% to
420 26%. The amount of K-feldspar ranges up to 2%, and the amount of plagioclase ranges from a few
421 percent up to 19%. Dolomite is present in trace amounts in the PA1 and PA2 samples of the
422 Pianello sections. Calcite occurs in all samples and it ranges from few percent up to 11% in the
423 upper portion of the Pianello section and throughout the Renali section. Variation of mineral
424 concentrations is related to the different source areas that influence the chemical and mineralogical
425 composition of the sediments.

426

427 6.2 Whole-rock geochemistry of mudstones

428 Major- and trace-element concentrations are listed in the Table 5. The studied mudstones have been
429 plotted in the classification diagram for terrigenous rocks (Fig. 9). The $\text{SiO}_2/\text{Al}_2\text{O}_3$ ratio, the most
430 commonly used parameter, reflects the relative abundance of quartz, feldspar and clay minerals
431 (e.g., Potter, 1978). The studied samples plot in the field of shale, toward the wacke field, thus
432 reflecting variation in the quartz–feldspars/mica ratio in the studied samples.

433 Geochemical compositions of the studied mud samples and the Post-Archean Australian Shales
434 (PAAS; Taylor and McLennan, 1985) were normalized to the to the Upper Continental Crust (UCC;
435 McLennan et al., 2006) (Fig. 10).

436 The mudstones are characterized by narrow compositional ranges for SiO_2 , Al_2O_3 , MnO and K_2O ,
437 which have concentrations close to those of the UCC (Fig. 10). Sodium and phosphorous are
438 strongly depleted relatively to UCC, but CaO is variable in concentration ranging from 1.65 (PA2)
439 to 7.03 wt.% (PA4). The observed Na_2O depletion is likely due to the burial history of these
440 samples, which promoted the formation of K-rich, mica-like clay minerals. The high CaO
441 concentrations are related to the carbonate minerals present in some samples of Renali area,
442 although the highest values of CaO have been also recorded within mudstones of Pianello area.
443 Magnesium is enriched relatively to UCC, ranging from to 5.73 (PA2) to 9,69 wt.% (MA1), and its
444 abundance is linked to occurrence of micas, as biotite and chlorite. Titanium and Fe_2O_3 values are
445 also high. The general trend of the observed UCC pattern shows similar variations with those
446 observed for the PAAS (Fig. 10).

447 In a ternary plot of SiO_2 (representing quartz), Al_2O_3 (representing mica/clay minerals), and CaO
448 (representing carbonates), the mudstones of Poggio Belvedere Mb. can be described as mixtures of
449 an aluminosilicate component with a small amount of carbonate phases (Fig. 11), although samples
450 from Renali area and PA4 from Pianello area show higher Ca content than the average shales
451 (PAAS).

452 These chemical associations and elemental variations are related to the mineralogical composition
453 of the studied mudstones, as shown above by the mineralogical analyses.

454

455 **7. Discussions**

456 *7.1 Provenance*

457 Detrital signatures of the Poggio Belvedere Mb. of the Macigno Fm. contain an abundance of
458 feldspars and coarse-grained phaneritic rock fragments, suggesting a source area of mostly plutonic
459 and metamorphic rocks, with minor mafic magmatic and sedimentary rocks. Various ratios of
460 feldspar, lithic fragment types, and quartz types in the sandstones reflect their transition between
461 basement uplift and a transitional continental provenance type (Figs. 6-8; e.g. Dickinson, 1985).
462 Sandstones of the Pianello Stratigraphic section of the Macigno Fm. are richer in F than those of the
463 Renali and Maestà stratigraphic sections. The latter sections have a Q-enrichment trend.
464 Referring to other diagrams, studied sandstones plot at the RgRm side in either RgRvRm and
465 RgRsRm diagrams (Critelli and Le Pera, 1994, 1995) and Lm in the LmLvLs diagram, confirming a
466 transition between plutonic and metamorphic rock fragments. In detail, Pianello and Renali
467 sandstones have an abundance of plutonic rock fragments, although some samples from the Renali
468 area have a mixture of plutonic and metamorphic detritus. The Maestà sandstones plot between
469 plutonic and metamorphic rock fragment field. This indicates a slight metamorphic trend.
470 Petrological data indicate that sandstones of Pianello Stratigraphic section represent the results of
471 prevalent drainage from an uplifted crystalline batholith with a dominance of granitoid rocks
472 (granodiorite and tonalite) and minor metamorphic rocks (gneiss and schist) ($Q_m/F = 1.3$; e.g.
473 Ibbeken and Schleyer, 1991), whereas sandstones of the Renali and Maestà Stratigraphic sections
474 reflect a provenance from a source area with a metamorphic-dominated basement (mica-schist, fine-
475 grained schist and phyllite. $Q_m/F \geq 2$; e.g. Ibbeken and Schleyer, 1991). This suggests the occurrence

476 of different pathways of drainage, resulting in a variation between a plutonic and metamorphic
477 contribution and in quartz-feldspar ratio, or provenance from different but similar source areas,
478 uplifted in the same time span. The main source area for the Macigno sandstones are inferred to be
479 from the Western-Central Alps, located north and northwest from the Macigno foreland basin
480 system.

481 The basement of the Western-Central Alps mainly consists of continental and oceanic-derived high
482 pressure metamorphic rocks (blueschist and greenschist facies) including ophiolites, marbles, calce-
483 schists, micas-schists, limestones, marls, and crystalline rocks, derived from external massifs (i.e.
484 Monte Rosa and Gran Paradiso Massifs and Dent Blanche complex). According to geological and
485 geodynamic data, based on age and amount of uplift, surface extent of source area, and volume of
486 uplifted rocks, the lithology of eroded rocks which were transferred to the Macigno foreland basin
487 system can be inferred from the Ivrea-Verbano block (Di Giulio, 1999). Moreover the plutonic
488 component of the Macigno Fm. sandstone could be related to less uplifted South Alpine crystalline
489 basement of the Central Southern Alps (e.g. Bigi et al., 1990; Di Giulio, 1999). Its prevalent
490 metamorphic composition, with only minor granite intrusions, is comparable with provenance
491 constraints based on the Macigno sandstone detrital modes (average value $Qm_{54}F_{29}Lt_{17}$; $Qm/F=1.9$)
492 studied in previous works (e.g. Di Giulio, 1999). The compositional results closely correspond with
493 detrital modes reported in overall sandstones of Poggio Belvedere Mb. of the present study (average
494 value: $Qm_{57}F_{34}Lt_9$; $Qm/F=1.85$), suggesting a general provenance from northwestward Alpine
495 metamorphic-dominated domains. The occurrence of a volcanic signal, and sedimentary detritus,
496 could be inferred from ophiolites and their sedimentary cover of Ligurian Nappe, although some
497 volcanic grains, which have felsic granular texture with plagioclase phenocrysts, might also indicate
498 a provenance from calc-alkaline trend volcanic arcs (i.e. Corsica-Sardinia block, Cornamusini et al.,
499 2002).

500 The W-oriented granitic-sourced sandstones of the Pianello area testify to the influence of
501 terrigenous material coming from a westernmost source area. The composition of these sandstones
502 could correspond with source rocks of the Corsica-Sardinia block as Cornamusini et alii (2002)
503 reported for the “Macigno Costiero” Fm.. However, the minor content of volcanic lithic fragments,
504 less abundant than in the “Macigno Costiero” Fm., and the location of Corsica-Sardinia during Late
505 Oligocene-Early Miocene, which was relatively far from Umbria-Tuscany foreland basin system
506 (Guerrera et al., 2015), also indicate the Alpine chain as W-derived crystalline source area (Fig. 12).
507 The provenance of plutonic-dominated sandstones from the less uplifted Central Alps crystalline
508 basement, located northwestward, do not explain the large amount of feldspars and phaneritic
509 plutonic rock fragments (e.g. Pianello Stratigraphic section), which are clearly more abundant than
510 other sandstones collected in the Macigno Apenninico (Valloni et al., 1991; Di Giulio, 1999; Dinelli
511 et al., 1999; Cornamusini, 2002; Barsella et al., 2009). In detail, the distance between the Central
512 Alpine crystalline basement and the Macigno basin of Trasimeno Lake area in the reconstructed
513 palaeogeographic framework (Fig. 12) is estimated to be several hundred of kilometres. On the
514 contrary, Pianello lobe-fringe sandstones (F4 to F7 facies; Mutti, 1992), originated by residual high-
515 density turbidites (Mutti, 1992), with the contribution of sudden decelerations of mud-rich turbidity
516 currents, as testified by several slurried divisions (Type 1 Beds by Tinterri and Muzzi-Magahalaes,
517 2011), represent the final result of depositional processes starting from a plutonic-dominated source
518 area that were very close to the Macigno foreland basin. The granite-sourced sandstones of Pianello
519 area is inferred to have been derived by drainage of the Monte Rosa and Gran Paradiso massifs and
520 Dent Blanche complex, located westward from the palaeo-Alps (Fig. 12), in which zircon fission-
521 track ages of exhumation (related to almost 40 ma) are closely related with those of the Macigno
522 sandstones (Dunkl et al., 2001).

523 The subordinate presence of extrabasinal carbonate detritus (e.g. Zuffa, 1985; Critelli et al., 2007)
524 may suggests an additional source area composed of ?Eocene to early Miocene limestones, as

525 shown by extrabasinal carbonate grains and fossils in the calciturbidites of the Renali area. The
526 occurrence of benthic macroforams suggests a provenance from an external shelf environment,
527 more probably located at the Adria-plate continental margin (Fig. 12), but wackestone-texture clasts
528 including planktonic foraminifers (*globigerinids*) indicate a clear signal from an inner basin. Similar
529 biofacies have been distinguished within calciturbidite and breccia levels of the Eocene-Oligocene
530 Scaglia Toscana Fm. in the Chianti Hills area, in which traction features indicate palaeoflows
531 towards the S and SW (Ielpi and Cornamusini, 2013) suggest a provenance from the Adria margin.
532 The variation among the LREEs (Light Rare Earth Elements; e.g., La and Ce) and the transition
533 elements (e.g., Co, Cr and Ni) is considered a useful indicator in provenance studies (e.g., Culler,
534 2000; Perri et al., 2012b). The range of elemental ratios (La+Ce/Co, La+Ce/Cr, and La+Ce/Ni; Tab.
535 5) of all samples studied suggests a provenance from fairly felsic rather than mafic source-areas
536 (e.g., Perri et al., 2012b). These ratio values do not exclude a supply of a mafic source,
537 predominantly for the Maestà section that shows lower La+Ce/Cr (on average 0.47) and La+Ce/Ni
538 (on average 0.79) than those of the Pianello and Renali sections (Tab. 5).
539 Generally, a low concentration of Cr and Ni indicates sediments derived from a felsic provenance,
540 whereas, higher content of these elements are mainly found in sediments derived from ultramafic
541 rocks (e.g., Wrafter and Graham, 1989; Armstrong-Altrin et al. 2004). Furthermore, the Cr/V ratio
542 is an index of the enrichment of Cr over the other ferromagnesian trace elements, whereas Y/Ni
543 monitors the general level of ferromagnesian trace elements (Ni) compared to a proxy for the HREE
544 (Y). Mafic–ultramafic sources tend to have high ferromagnesian abundances; such a provenance
545 would result in a decrease in Y/Ni ratios and an increase in Cr/V ratios (e.g., Hiscott 1984;
546 McLennan et al. 1993). The Cr/V vs. Y/Ni diagram (Hiscott, 1984) indicates a mixed source for the
547 studied samples. In particular, the sediments are derived from a mainly felsic source area with a
548 supply of a mafic source, predominantly for the Maestà section that shows Cr/V values ranging
549 from 1.15 to 3.36 (Fig. 13). The V-Ni-La*10 diagram also suggests a similar provenance (e.g.

550 [Bracciali et al., 2007](#); [Perri et al., 2011b](#)) ([Fig. 14](#)), where the studied samples fall in an area related
551 to provenance from a mixed source, mainly characterized by felsic rocks with a supply of mafic
552 rocks. The mafic supply is probably related to the Ligurian ophiolites.

553

554 *7.2 Source-area weathering*

555 The evaluation of the source area weathering processes is mainly related to the **variation** of alkali
556 and alkaline-earth elements in siliciclastic sediments. The Chemical Index of Alteration (CIA;
557 [Nesbitt and Young 1982](#)) is one of the most used **indices** to quantify the degree of source area
558 weathering. Furthermore, when the sediments **contain a** high proportion of CaO, an alternative
559 index of alteration CIA', expressed as molar volumes of $[Al/(Al+Na+K)] \times 100$, has **also** used (e.g.,
560 [Perri et al., 2014, 2015](#)). The chemical compositions of studied mudstones are plotted as molar
561 proportions within the A-CN-K and A-N-K diagrams. The CIA values of **the** studied samples are
562 quite homogeneous (average = 66.4) **with** low-moderate **values** and in the A-CN-K triangular
563 diagram the samples plot in a tight group on the A-K join close to the illite-muscovite point ([Fig.](#)
564 [15A](#)), suggesting low-moderate weathering conditions. Furthermore, the CIA' values of **the**
565 **mudrocks** (average = 69.7) are quite similar to the CIA, typical of low-moderate weathering
566 conditions. **In** the A-CN-K triangular diagram the samples plot in a tight group on the A-K join
567 close to the illite-muscovite point ([Fig. 15B](#)). Micas (both illite and muscovite) are the dominant
568 phyllosilicates occurring within the studied mudstones.

569 Simple ratios such as Al/K and Rb/K (e.g., [Schneider et al., 1997](#); [Roy et al., 2008](#)), characterized
570 by elements with contrasting mobility in the supracrustal environment, have been also used as a
571 broad measure of weathering. Generally, high Al/K ratios are typical of sediments enriched in
572 kaolinite, an important product of intensive weathering, over feldspar (or other K-bearing minerals).
573 The Al/K ratios are low and constant (average= 4.47 ± 0.41) for all the studied sediments suggesting
574 low-moderate weathering and no important fluctuations in weathering intensity, as also shown in

575 the A-CN-K and A-N-K diagrams (Fig. 15). Furthermore, Rb/K ratios have been used to monitor
576 source area weathering, where K is preferentially leached over Rb with increased intensity of
577 weathering (Wronkiewicz and Condie, 1989, 1990; Peltola et al., 2008). Very low and
578 homogeneous values of Rb/K ratios (<0.006) are found in the studied sediments, indicating weak to
579 moderate weathering in a warm-humid climate (typical of the Mediterranean area) with minimal or
580 negligible variations over time (e.g., Mongelli et al., 2012 and references therein).

581

582 *7.3 Sorting, transport and recycling*

583 Generally, transport and deposition of terrigenous sediments involve mechanical sorting, that may
584 affect the chemical composition of terrigenous sediments and, thus, the distribution of source area
585 weathering and provenance proxies (e.g., Mongelli et al., 2006; Perri et al., 2011a, 2012a, 2014).

586 Aluminum, titanium and zirconium are the major and minor elements generally considered the least
587 mobile during chemical weathering (e.g. Perri et al., 2008a). Resistant minerals such as zircon,
588 rutile and ilmenite generally host significant amounts of Ti and Zr. Variations in these elements are
589 expressed in the Al–Ti–Zr ternary plot (García et al., 1994) that can highlight the possible effect of
590 zircon addition mainly related to sorting and recycling processes. The studied mudstones plot in a
591 tight area in the middle of the $15 \cdot \text{Al}_2\text{O}_3\text{-Zr-}300 \cdot \text{TiO}_2$ diagram (Fig. 16), and they are mostly
592 characterized by homogeneous values in the $\text{Al}_2\text{O}_3/\text{Zr}$ ratio that could be due to poor recycling
593 effects without a marked Zr enrichment (e.g., Perri et al., 2008a, 2011a; Caracciolo et al., 2011 and
594 references therein).

595 The Index of Compositional Variability (Cox et al., 1995) has been generally used as a measure of
596 compositional maturity. Immature mudstones, containing a high proportion of silicates other than
597 clays, commonly show high values of this index ($\text{ICV} > 1$), whereas mature mudstones, depleted in
598 silicates other than clays, generally show low ICV values ($\text{ICV} < 1$). Furthermore, immature
599 mudrocks tend to be found in tectonically active settings and are characteristically first-cycle

600 deposits (Van de Kamp and Leake, 1985), whereas mature mudrocks characterize tectonically
601 quiescent or cratonic environments (Weaver, 1989) where sediment recycling is active. The studied
602 sediments show $ICV > 1$ (average = 1.51 ± 0.26) typical of first cycle, immature sediments where
603 chemical weathering plays a minor role consistent with the medium-low CIA and CIA' values.
604 Furthermore, the ICV values are also consistent with the sample distribution within the Al–Ti–Zr
605 ternary plot that exclude recycling effects for the studied sediments, suggesting a very rapid
606 transport in a depositional area close to the source(s). Such geochemical interpretation is totally
607 compatible with ichnocoenosis, reported by Monaco and Trecci (2014). In fact the very large
608 abundance of endichnial *Halopoa* (*H. embricata* and *H. var. fucusopsis*) suggests a basin floor
609 environment rich in organic matter (i.e. phyto detritus) and diversified geochemical elements,
610 extremely important to a proliferation of this ichnotaxon close to an alimentation source. Moreover
611 the missing of *Avetoichnus luisae*, *Zoophycos* and *Nereites* trace fossils (see the ichnosubfacies at
612 *Nereites*), occurring in the underlying Scaglia Toscana Fm. and in the overlying Marnoso Arenacea
613 Fm., typical of distal deep-water areas, testifies to a very high sedimentation rate and the proximity
614 of the depositional area to the source area. The differences among ichnotaxa is minimal in the three
615 studied stratigraphic sections. However a slightly increasing on graphoglyptid abundance and
616 diversification can be noted in the upper Renali and Maestà sections differently to the Pianello
617 section (e.g. *Paleodictyon* and *Spirorhaphé*). This could be explained due to a progressive
618 deepening of the basin plain environment.

619 The textural characteristics of the studied sandstones show moderate to low sorting, low degree of
620 roundness of grains, and lack of altered quartz grains, confirming either poor recycling or closeness
621 to the source area. However, sandstones at the Maestà Stratigraphic section are well sorted,
622 indicating the settling of a fine-grained turbidite flow (F9 facies) in farthestmost portion of the
623 foredeep basin. Furthermore, the good sphericity of some clasts, their general equant-prolate shape,
624 and their poor degree of flattening in outer lobe facies (F5-F7 facies in Pianello and Renali

625 Stratigraphic sections) suggest that grains were initially reworked in a deltaic/fluvial sedimentary
626 system and then resedimented into a deep-sea basin (e.g. [Sames, 1966](#); [Walker, 1975](#)). Finally in
627 Pianello Stratigraphic section the occurrence of well preserved continental vegetal remains and
628 several slurried divisions indicate fast and sudden transport (e.g. hyperpicnal plumes), from a close
629 source-area which were more probably located westward, as well indicated by W-oriented sandy
630 debris flows.

631

632 **8. Conclusions**

633 The Macigno **Fm.** sandstones, sampled in Poggio Belvedere **Mb.** in the Trasimeno Lake area, show
634 a general quartzofeldspathic composition, but with some differences in the quartz/feldspar ratio
635 (Qm/F) and in the composition of either phaneritic rock fragments and fine-grained lithic fraction.

636 The abundance of feldspars (lower Qm/F) and phaneritic plutonic and discrete occurrence of high-
637 grade metamorphic rock fragments in lobe-fringe facies sandstones (F5-F7 facies) of **the** Pianello
638 Stratigraphic section match those found in some granitoid-source modern sands of Calabria
639 ([Ibbeken and Schleyer, 1991](#); [Perri et al., 2012b](#)). These data, coupled with **evidence** of W-oriented
640 flows, suggest a provenance from a granitoid-dominated batholith, and indicate **the external massifs**
641 **of the Western Alps (Monte Rosa and Gran Paradiso massifs, Dent Blanche complex) as a potential**
642 **plutonic and high-grade metamorphic source area.**

643 The overall NW-SE oriented fine-grained turbidites of **the** basin plain facies (F8 and F9a-b facies)
644 and lobe-fringe sandstones of **the** Maestà Stratigraphic section have **a** higher Qm/F ratio **than those**
645 **of Pianello Stratigraphic section. They** are characterized by **a** lower plutonic content, metamorphic
646 lithic fragments, **a** fine-grained, low-medium grade metamorphic component, and **subordinate**
647 volcanic lithic fragments in **a** similar amount with those studied previously in the sandstones of **the**
648 Macigno **Fm.** ([Di Giulio et al., 1999](#) and [Barsella et al., 2009](#)) and in metamorphic-source modern

649 sands of Calabria (Ibbeken and Schleyer, 1991). These data mainly suggest a provenance from a
650 metamorphic basement and a crystalline batholith that can be respectively identified with the Ivrea-
651 Verbano block in Central-Western Alps and South Alpine crystalline basement in the Central
652 Southern Alps (Di Giulio, 1999).

653 Volcanic and metavolcanic grains, coupled with Cr and Ni enrichment, mainly indicate a
654 provenance from an ophiolitic unit and overlying sedimentary cover of the Ligurian Nappe. An
655 enrichment of Nb and a peculiar occurrence of volcanic fragments with felsic granular fabric
656 including plagioclase and quartz phenocrysts could be related to calco-alkaline rhyolites which
657 characterize the Late Oligo-Early Miocene volcanic arc that originated by subduction of the Adria
658 microplate beneath the eastern margin of Mesomediterranean continent (Guerrera et al., 2015).

659 Finally the presence of East-derived calciturbidites in the Renali area including a typical biofacies
660 of external shallow-water platform indicate a provenance from the Adria margin (Central
661 Apennines).

662 This detailed petrology coupled with sedimentological data (Monaco and Trecci, 2014) allows a
663 better understanding of the spatial compositional evolution of the Macigno Fm., in agreement with
664 the model for migrating foredeep basins proposed by Ricci Lucchi (1986). Firstly sedimentation
665 developed in the westernmost internal zones, which were transversally fed mainly by the crystalline
666 basement of external massifs. During the migration of the orogenic front and foredeep basin, the
667 transversal feeders were substituted by longitudinal basin feeders from Western-Central Alps that
668 were supplied with material similar to those from external massifs but with minor plutonic and
669 high-grade metamorphic fragments. In the Late Oligocene-Early Miocene time interval, the
670 Trasimeno Lake area was probably located in the distal external zones of Macigno foredeep that
671 received terrigenous material firstly from the W-SW-oriented external massifs feeders (Pianello and
672 lower Renali areas) and successively from the NW-oriented Central Alpine and S-oriented
673 Apennine feeders (upper Renali and Maestà areas). Also ichnocoenoses seem to confirm this

674 evolutionary trend. A similar compositional trend could be accounted for the Macigno Fm. in
675 Northwestern Tuscany (Abetone area) analyzed by [Bruni et alii \(2007\)](#).

676 The geochemistry and mineralogy of **Late Oligocene-Early** Miocene deep-sea mudstones from
677 Poggio Belvedere stratigraphic section of the Macigno **Fm.** suggest interesting palaeoclimatic and
678 paleoweathering indications. The **mudrocks** have concentrations very similar to those of the UCC
679 ([McLennan et al. 2006](#)) for Si, Al, Fe, Zr, K, whereas, Ca, Na, P, Ba and Sr are strongly depleted.
680 Cesium and rubidium are slight enriched to the UCC and show a positive correlation with
681 potassium, suggesting these trace elements are mostly hosted by dioctahedral mica-like clay
682 minerals. This in turn indicates that illite and illitic minerals (I/S mixed layers) have played an
683 important role in the distribution of elements in these rocks since these minerals are abundant in the
684 studied samples. Furthermore, the mudstones fall in a tight group on the A-K join, in the A-CN-K
685 triangular diagram, close to the muscovite point, in agreement with the mineralogical data. **The** Cr,
686 Ni and Nb **concentrations** are enriched to the UCC, and indicate **a trace of a mafic source**.

687 **The source area for the studied mudstones should have similar features to those of Western-Central**
688 **Alps and crystalline external massifs basement**, which are predominantly composed of felsic rocks
689 with non-trivial amounts of mafic rocks. Geochemical proxies consistently suggest a felsic nature of
690 the source area, with a minor but not negligible supply from mafic rocks that increased in the
691 younger deposits (Maestà Stratigraphic section).

692 **Both** the CIA and the CIA' proxies suggest low-moderate weathering at the source area. The
693 studied sediments seems to be affected by brief reworking in fluvial/deltaic zone and poor recycling
694 processes and, as a consequence, it is likely these proxies monitor cumulative effects of weathering
695 (e.g., [Mongelli et al. 2006](#); [Critelli et al. 2008](#); [Perri et al. 2008a, 2008b](#)).

696 The chemical weathering of such rocks under **a** humid climate season would produce an initial
697 illitization of silicate minerals. Moreover, palaeocurrent analysis clearly indicates that terrigenous

698 terrigenous rocks derived from rapid erosion of highlands located to the N, NW, W and E of the
699 present-day outcrops of the Trasimeno Lake area.

Acknowledgements

U. Amendola was supported by the “;CARICAL Foundation”; in Cosenza, Italy. Work supported by the MIUR-UNICAL Project (Relationships between Tectonic Accretion, Volcanism and Clastic Sedimentation within the Circum-Mediterranean Orogenic Belts, 2006e2011; Resp. S. Critelli). We are grateful to reviewers Manuel Martín-Martín, an anonymous reviewer and the Associate Editor Massimo Zecchin for reviews, helpful discussions, and comments on an earlier version of the manuscript.

References

- Andreozzi, M., Di Giulio, A., 1994. Stratigraphy and petrography of the M. Cervarola Sandstones in the type area, Modena Province. *Mem. Soc. Geol. It.* 48, 351–360.
- Armstrong-Altrin, J.S., Lee, Y.I., Verma, S.P., Ramasamy, S., 2004. Geochemistry of sandstones from the upper Miocene Kudankulam Fm., southern India: Implications for provenance, weathering, and tectonic setting. *J Sed Res* 74, 285–297. DOI: [10.1306/082803740285](https://doi.org/10.1306/082803740285)
- Aruta, G., 1994. Stratigraphy of the Falterona and Cervarola sandstones in the Cortona area (Arezzo, Northern Apennines). *Mem. Soc. Geol. It.*, 48, 361-369.
- Aruta, G., Pandeli, E., 1995. Lithostratigraphy of the M. Cervarola - M. Falterona Fm. between Arezzo and Trasimeno Lake (Tuscan-Umbria, Northern Apennines, Italy). *Giorn. Geol.*, serie 3a, 57 (1-2), 131-157.
- Aruta, G., Bruni, P., Cipriani, N., Pandeli, E., 1998. The siliciclastic turbidite sequences of the Tuscan Domain in the Val di Chiana-Val Tiberina area (eastern Tuscany and north-western Umbria). *Mem. Soc. Geol. It.*, 52, 579-593.
- Barsella, M., Boscherini, A., Botti, F., Marroni, M., Meneghini, F., Motti, A., Palandri, S., and Pandolfi, L., 2009. Oligocene-Miocene foredeep deposits in the Lake Trasimeno area (Central Italy): insights into the evolution of the Northern Apennines. *Ital. J. Geosci. (Boll. Soc. Geol.It.)*, Vol. 128, No. 2, pp. 341-352. DOI: [10.3301/IJG.2009.128.2.341](https://doi.org/10.3301/IJG.2009.128.2.341)
- Basu, A., 1985. Reading provenance from detrital quartz. In: Zuffa, G.G. (Ed.), *Provenance of Arenites*. D. Reidel Publishing, Boston, pp. 231–247.
- Bauluz, B., Mayayo, M.J., Fernandez-Nieto, C., Gonzalez Lopez, J.M., 2000. Geochemistry of Precambrian and Paleozoic siliciclastic rocks from the Iberian Range (NE Spain): implications for source-area weathering, sorting, provenance, and tectonic setting. *Chemical Geology* 168, 135–150. DOI: [10.1016/S0009-2541\(00\)00192-3](https://doi.org/10.1016/S0009-2541(00)00192-3)

- Bigi, G., Castellarin, A., Coli, M., Dal Piaz, G.V, Sartori, R., Scandone, P., Vai, G.B., 1990. Structural model of Italy, scale 1:500,000, sheet n. 1. S.E.L.C.A. press, Florence.
- Boccaletti, M., Calamita, F., Deiana, R., Gelati, R., Massari, F., Moratti, G., Ricci Lucchi, F., 1990. Migrating foredeep-thrust belt system in the northern Apennines and southern Alps. *Palaeogeogr Palaeoclimatol Palaeoecol* 77, 3–14. DOI: [10.1016/S0009-2541\(00\)00192-3](https://doi.org/10.1016/S0009-2541(00)00192-3)
- Bracciali, L., Marroni, M., Luca, P., Sergio, R., 2007. Geochemistry and petrography of Western Tethys Cretaceous sedimentary covers (Corsica and Northern Apennines): From source areas to configuration of margins. *GSA Spec. Pap.*, 420, 73-93. DOI: [10.1130/2006.2420\(06\)](https://doi.org/10.1130/2006.2420(06))
- Brozzetti, F., 2007. The Umbria Preapennines in the Monte Santa Maria Tiberina area: a new geological map with stratigraphic and structural notes. *Boll. Soc. Geol. It.*, 126 (3), 511-529.
- Bruni, P., Pandeli, E., 1980. Torbiditi calcaree nel Macigno e nelle Arenarie del Cervarola nell'area del Pratomagno e del Falterona (Appennino settentrionale). *Mem. Soc. Geol. It.*, 21, 217-230.
- Bruni, P., Pandeli, E., Nebbiai, M., 2007. Petrographic analysis in regional geology interpretation: Case history of the Macigno (northern Apennines), in Arribas J., Critelli S. and Johnsson M., editors, *Sedimentary Provenance: Petrographic and Geochemical Perspectives*. Geological Society of America Special Paper 420, p. 95-105. DOI: [10.1130/2006.2420\(07\)](https://doi.org/10.1130/2006.2420(07))
- Canuti, P., Focardi, P., Sestini, G., 1965. Stratigrafia, correlazione e genesi degli Scisti Policromi dei monti del Chianti (Toscana). *Boll. Soc. Geol. It., Vol. Spec.*, 84, 93-166.
- Caracciolo, L., Le Pera, E., Muto, F., Perri, F., 2011. Sandstone petrology and mudstone geochemistry of the Peruc–Korycany Fm. (Bohemian Cretaceous Basin, Czech Republic). *Int. Geo. Rev.* 53, 1003–1031. DOI: [10.1080/00206810903429011](https://doi.org/10.1080/00206810903429011)
- Castellarin, A., 1992. Introduzione alla progettazione del profilo CROP. *Studi Geol. Camerti, Spec.* Vol. 1992 (2), 9–15.

- Cavalcante, F., Fiore, S., Lettino, A., Piccarret, G., Tateo, F., 2007. Illite–smectite mixed layers in sicilide shales and piggy-back deposits of the Gorgoglione Fm. (Southern Apennines): geological inferences geodynamic implications. *Bol. Soc. Geol. It.* 126, 241–254.
- Centamore, E., Fumanti, F., Nisio, S., 2002, The Central Northern Apennines geological evolution from Triassic to Neogene time: *Boll. Soc. Geol. It., Spec. Vol. N°1*: 181-197.
- Condie, K.C., Noll, P.D.J., Conway, C.M., 1992. Geochemical and detrital mode evidence fortwosourcesofearlyProterozoicsedimentaryrocksfromtheTontoBasinSupergroup, central Arizona. *Sed. Geol.* 77, 51–76. DOI: [10.1016/0037-0738\(92\)90103-X](https://doi.org/10.1016/0037-0738(92)90103-X)
- Condie, K.C., Lee,D., Farmer,G.L., 2001.Tectonic setting and provenance of the Neoproterozoic Uinta Mountain and Big Cottonwood groups, northern Utah: constraints from geochemistry, Nd isotopes, and detrital modes. *Sed. Geol.* 141, 443–464. DOI: [10.1016/S0037-0738\(01\)00086-0](https://doi.org/10.1016/S0037-0738(01)00086-0)
- Cornamusini, G., 2002. Compositional evolution of the Macigno Fm. of southern Tuscany along a transect from the Tuscan coast to the Chianti Hills. *Boll. Soc. Geol. It., volume speciale n.1*, 365-374.
- Cornamusini, G., Elter, F. M., Sandrelli, F., 2002. The Corsica–Sardinia Massif as source area for the early northern Apennines foredeep system: evidence from debris flows in the “Macigno costiero” (Late Oligocene, Italy). *Int J Earth Sci (Geol Rundsch)* 91, 280–290. DOI [10.1007/s005310100212](https://doi.org/10.1007/s005310100212)
- Cox, R., Lowe, D., Cullers, R.L., 1995. The Influence of Sediment Recycling and Basement Composition on Evolution of Mudrock Chemistry in Southwestern United States. *Geochim. Cosmochim. Acta*, 59, 2919-2940. DOI: [10.1016/0016-7037\(95\)00185-9](https://doi.org/10.1016/0016-7037(95)00185-9)
- Critelli S., 1993. Sandstone detrital modes in the Paleogene Liguride Complex, accretionary wedge of the Southern Apennines (Italy). *J. Sed. Res.*, v. 63, p. 464-476. DOI: [10.1306/D4267B27-2B26-11D7-8648000102C1865D](https://doi.org/10.1306/D4267B27-2B26-11D7-8648000102C1865D)

- Critelli, S., 1999. The interplay of lithospheric flexure and thrust accommodation in forming stratigraphic sequences in the southern Apennines foreland basin system, Italy. *Accademia Nazionale dei Lincei, Rendiconti Lincei Scienze Fisiche e Naturali*, v. 10, p. 257-326.
- Critelli, S., Ingersoll, R.V., 1995. Interpretation of neovolcanic versus palaeovolcanic sand grains: an example from Miocene deep-marine sandstone of the Topanga Group (southern California). *Sedimentology* 42, 783–804. DOI: [10.1111/j.1365-3091.1995.tb00409.x](https://doi.org/10.1111/j.1365-3091.1995.tb00409.x)
- Critelli, S., Le Pera, E., 1994. Detrital modes and provenance of Miocene sandstones and modern sands of the Southern Apennines thrust-top basins (Italy). *J. Sed. Res.* 64, 824–835.
- Critelli, S., Le Pera, E., 1995. Tectonic evolution of the Southern Apennines thrust-belt (Italy) as reflected in modal compositions of Cenozoic sandstone. *J. Geol.* 103, 95-105.
- Critelli, S., De Rosa, R., Platt, J.P., 1990. Sandstone detrital modes in the Makran accretionary wedge, southwest Pakistan: Implications for tectonic setting and long-distance turbidite transportation. *Sed. Geol.*, v. 68, p. 241-260. DOI: [10.1016/0037-0738\(90\)90013-J](https://doi.org/10.1016/0037-0738(90)90013-J)
- Critelli S., Le Pera E., Galluzzo F., Milli S., Moscatelli M., Perrotta S., Santantonio M., 2007. Interpreting siliciclastic-carbonate detrital modes in Foreland Basin Systems: an example from Upper Miocene arenites of the Central Apennines, Italy, in Arribas J., Critelli S. and Johnsson M., editors, *Sedimentary Provenance: Petrographic and Geochemical Perspectives*. GSA Special Paper 420, p. 107-133. DOI: [10.1130/2006.2420\(08\)](https://doi.org/10.1130/2006.2420(08))
- Critelli, S., Mongelli, G., Perri, F., Martin-Algarra, A., Martin-Martin, M., Perrone, V., Dominici, R., Sonnino, M., Zaghoul, M.N., 2008. Compositional and geochemical signatures for the sedimentary evolution of the Middle Triassic–Lower Jurassic continental redbeds from western-central Mediterranean Alpine chains. *J. Geol.* 116, 375–386. DOI: [10.1086/588833](https://doi.org/10.1086/588833)
- Cullers, R.L., 2000. The geochemistry of shales, siltstones and sandstones of Pennsylvanian–Permian age, Colorado, USA: implications for provenance and metamorphic studies. *Lithos* 51, 181-203.

Damiani, A.V., Faramondi, S., Nocchi-Lucarelli, M., Pannuzi, L., 1987. Biocronostratigrafia delle unità litologiche costituenti “l’insieme varicolore” affiorante tra la Val di Chiana ed il fiume Tevere (Italia centrale). *Boll. Serv. Geol. d’It.*, Roma, 106, 109-160.

De Capoa et al. (2015) Swiss J. geosc.

Di Giulio, A., 1999. Mass transfer from the Alps to the Apennines: volumetric constraints in the provenance study of the Macigno–Modino source–basin system, Chattian–Aquitania, northwestern Italy. *Sed. Geol.* 124, 69–80. DOI: [10.1016/S0037-0738\(98\)00121-3](https://doi.org/10.1016/S0037-0738(98)00121-3)

Dickinson, W.R., 1970. Interpreting detrital modes of greywacke and arkose. *Journal of Sed. Petr.* 40, 695–707.

Dickinson, W.R., 1985. Interpreting provenance relations from detrital modes of sandstones. In: Zuffa, G.G. (Ed.), *Provenance of Arenites*. North Atlantic Treaty Organization Advanced Study Institute Series, 148. D. Reidel, Dordrecht, The Netherlands, pp. 331–361. DOI: [10.1007/978-94-017-2809-6_15](https://doi.org/10.1007/978-94-017-2809-6_15)

Dinelli, E., Lucchini, F., Mordenti, A., and Paganelli, L., 1999. Geochemistry of Oligocene–Miocene sandstones of the northern Apennines (Italy) and evolution of chemical features in relation to provenance changes. *Sed. Geol.* 127, 193–207. DOI: [10.1016/S0037-0738\(99\)00049-4](https://doi.org/10.1016/S0037-0738(99)00049-4)

Dunham, R.J., 1962. Classification of carbonate rocks according to depositional texture. In Ham, W.E. *Classification of carbonate rocks*. AAPG Memoir. 1. pp.108–121.

Dunkl, I., Di Giulio, A., Kuhlemann, J., 2001. Combination of single-grain fission-track chronology and morphological analysis of detrital zircon crystals in provenance studies-sources of the Macigno Fm. (Apennines, Italy). *J. Sed. Res.*, vol. 71, n. 4, p. 516-525. DOI: [10.1306/102900710516](https://doi.org/10.1306/102900710516)

Einsele, G., 1991. Submarine mass flow deposits and turbidites. In: Einsele G., Ricken W. & Seilacher A. (Eds.), *Cycles and Events in Stratigraphy*. Springer, Berlin, 313-339.

- Embry, A.F. III, Klovan, J.S., 1971. A Late Devonian reef tract on northeastern Banks Island, N.W.T. Bulletin of Canadian Petroleum Geology vol. 4, p. 730-781.
- Flanagan, F.J., 1976. Descriptions and Analyses of Eight New USGS Rock Standards. U.S. Geological Survey Professional Paper 840, Washington, 192 p.
- Folk, R. L., 1968. Petrology of Sedimentary Rocks. Austin, University of Texas Publication, 170 p.
- Gandolfi, G., Paganelli, L., Zuffa, G.G., 1983. Petrology and dispersal pattern in the Marnoso-arenacea Fm. (Miocene, Northern Apennines). J. Sed. Petr. 53, 493-507. DOI: [10.1306/212F8215-2B24-11D7-8648000102C1865D](https://doi.org/10.1306/212F8215-2B24-11D7-8648000102C1865D)
- García, D., Fontelles, M., Moutte, J., 1994. Sedimentary fractionations between Al, Ti, and Zr and the genesis of strongly peraluminous granites. Journal of Geology 102, 411–422.
- Gazzi, P., 1966. Le arenarie del Flysch sopracretaceo dell'Appennino modenese; correlazioni con il Flysch di Monghidoro. Mineralogica et Petrografica Acta 12, 69–97.
- Graham, S. A., Ingersoll, R. V., Dickinson, W. R., 1976. Common provenance for lithic grains in Carboniferous sandstones from Ouachita Mountains and Black Warrior basin. Jour. Sed. Petrology, v. 46, p. 620-632. DOI: [10.1306/212F7009-2B24-11D7-8648000102C1865D](https://doi.org/10.1306/212F7009-2B24-11D7-8648000102C1865D)
- Guerrera et al., 2012 (Swiss J. Geosciences, 105, 3, 325-341);
- Guerrera et al., 2012 (24, 34-41);
- Guerrera et al., 2013 (TerraNova, 25, 119-129)
- Guerrera & Martín-Martín, 2014 (Bull Soc Geol Fr, 185, 5, 329-341)
- Guerrera F., Martín-Martín, M., Raffaelli, G., Tramontana, M., 2015. The Early Miocene “Bisciario volcaniclastic event” (northern Apennines, Italy): a key study for the geodynamic evolution of the central-western Mediterranean. Int. J. Earth Sci. (Geol. Rundsch), in press. DOI [10.1007/s00531-014-1131-5](https://doi.org/10.1007/s00531-014-1131-5)
- Harnois, L., 1988. The C.I.W. index: a new chemical index of weathering. Sed. Geol. 55, 319–322. DOI: [10.1007/s00531-014-1131-5](https://doi.org/10.1007/s00531-014-1131-5)

- Herron, M.M., 1988. Geochemical classification of terrigenous sands and shales from core or log data. *J. Sed. Petr.* 58, 820–829. DOI:10.1306/212F8E77-2B24-11D7-8648000102C1865D
- Hill, K.C., Hayward, A.B., 1988. Structural constraints on the Tertiary plate tectonic evolution of Italy. *Mar. Pet. Geol.* 5, 2–16. DOI: 10.1016/0264-8172(88)90036-0
- Hiscott, R.N., 1984. Ophiolitic source rocks for Taconic-age flysch: trace element evidence. *Geol. Soc. Am.* 95, 1261–1267. DOI: 10.1130/0016-7606(1984)95<1261:OSRFTF>2.0.CO;2
- Ibbeken, H., Schleyer, R., 1991. *Source and Sediment. A Case Study of Provenance and Mass Balance at an Active Plate Margin (Calabria, Southern Italy)*. Springer, Berlin.
- Ielpi, A. and Cornamusini, G., 2013. An outer ramp to basin plain transect: Interacting pelagic and calciturbidite deposition in the Eocene–Oligocene of the Tuscan Domain, Adria Microplate (Italy). *Sed. Geol.*, 294: 83–104. DOI: 10.1016/j.sedgeo.2013.05.010
- Ingersoll, R.V., Suczek, C.A., 1979. Petrology and provenance of Neogene Sand from Nicobar and Bengalfans, DSDP sites 211 and 218. *J. Sed. Petr.* 49, 1217–1228. DOI:10.1306/212F78F1-2B24-11D7-8648000102C1865D
- Ingersoll, R.V., Bullard, T.F., Ford, R.L., Grimm, J.P., Pickle, J.D., Sares, S.W., 1984. The effect of grain size on detrital modes: a test of the Gazzi–Dickinson point-counting method. *J. Sed. Petr.* 54, 103–116. DOI: 10.1306/212F83B9-2B24-11D7-8648000102C1865D
- Johnsson, M.J., 1993. The system controlling the composition of clastic sediments. In: Johnsson, M.J., Basu, A. (Eds.), *Processes controlling the composition of clastic sediments: GSA Special Paper, 284*, pp. 1–19. DOI: 10.1130/SPE284-p1
- Krumm, S., 1996. WINFIT 1.2: version of November 1996 (The Erlangen geological and mineralogical software collection) of “WINFIT 1.0: a public domain program for interactive profile-analysis under WINDOWS”. XIII Conference on Clay Mineralogy and Petrology, Praha, 1994: *Acta Universitatis Carolinae Geologica*, 38, pp. 253–261.

- McLennan, S.M., Taylor, S.R., Hemming, S.R., 2006. Composition, differentiation, and evolution of continental crust: constraints from sedimentary rocks and heat flow. In: Brown M, Rushmer T (eds) Evolution and differentiation of the continental crust. Cambridge University Press, Cambridge, pp 92–134.
- Milighetti, M., Monaco, P. and Checconi, A., 2009. Caratteristiche sedimentologico-ichnologiche delle unità silicoclastiche oligo-mioceniche nel transetto Pratomagno-Verghereto, Appennino Settentrionale. *Annali dell'Università degli Studi di Ferrara, Museologia Scientifica e Naturalistica*, 5: 23-129.
- Monaco, P., Trecci, T., 2014. Ichnocoenoses in the Macigno turbidite basin system, Lower Miocene, Trasimeno (Umbrian Apennines, Italy). *Ital. J. Geo.* 133, 116-130. DOI: [10.3301/IJG.2013.18](https://doi.org/10.3301/IJG.2013.18)
- Monaco, P., Uchman, A., 1999. Deep-sea ichnoassemblages and ichnofabrics of the Eocene Scisti varicolori beds in the Trasimeno area, western Umbria, Italy. In: A. Farinacci & A. R. Lord (Editors), *Depositional Episodes and Bioevents. Paleopelagos*, Univ. La Sapienza, Spec. Publ., Roma, pp. 39-52.
- Monaco, P., Milighetti, M., Checconi, A., 2009. Ichnocoenoses in the Oligocene to Miocene foredeep basins (Northern Apennines, central Italy) and their relation to turbidite deposition. *Acta Geol. Polon.*, 60 (1), 53-70.
- Monaco, P., Trecci, T., Uchman, A., 2012. Taphonomy and ichnofabric of the trace fossil *Avetoichnus luisae* Uchman & Rattazzi, 2011 in Paleogene deep-sea fine-grained turbidites: examples from Italy, Poland and Spain. *Boll. Soc. Paleont. Ital.*, 51(1), 1-16.
- Mongelli, G., Critelli, S., Perri, F., Sonnino, M., Perrone, V., 2006. Sedimentary recycling, provenance and paleoweathering from chemistry and mineralogy of Mesozoic continental redbed mudrocks, Peloritani Mountains, Southern Italy. *Geochem. J.* 40, 197–209.

- Mongelli, G., Mameli, P., Oggiano, G., Sinisi, R., 2012. Messinian palaeoclimate and palaeo-environment in the western Mediterranean realm: insights from the geochemistry of continental deposits of NW Sardinia (Italy). *Int. Geol. Rev.*, 54, 971-990. DOI: [10.1080/00206814.2011.588823](https://doi.org/10.1080/00206814.2011.588823)
- Mutti, E., 1992. Turbitite sandstones. AGIP S.p.a. (Eds.), S. Donato milanese, pp. 275.
- Muzzi Magalhaes P., Tinterri, R., 2010. Stratigraphy and depositional setting of slurry and contained (reflected) beds in the Marnoso-arenacea Fm. (Langhian Serravallian) Northern Apennines, Italy. *Sedimentology* 57, 1685–1720. DOI: [10.1111/j.1365-3091.2010.01160.x](https://doi.org/10.1111/j.1365-3091.2010.01160.x)
- Nesbitt, H.W., 1992. Diagenesis and metamorphism of weathering profiles, with emphasis on Precambrian paleosols. In: Martini IP, Chesworth W (eds) *Weathering, soils and paleosols*. Elsevier, Amsterdam, pp. 127–152. ISBN: [978-0-444-89198-3](https://www.isbn-international.org/product/978-0-444-89198-3)
- Nesbitt, H.W., Young, G.M., 1982. Early Proterozoic climates and plate motions inferred from major element chemistry of lutites. *Nature* 299, 715–717. DOI: [10.1038/299715a0](https://doi.org/10.1038/299715a0)
- Nesbitt, H.W., Young, G.M., McLennan, S.M., Keays, R.R., 1996. Effects of chemical weathering and sorting on the petrogenesis of siliciclastic sediments, with implications for provenance studies. *Journal of Geology* 104, 525–542.
- Peltola, P., Brun, C., Strom, M., Tomilia, O., 2008. High K/Rb ratios in stream waters. Exploring plant litter decay, ground water and lithology as potential controlling mechanisms. *Chem. Geol.*, 257, 92-100. DOI:[10.1016/j.chemgeo.2008.08.009](https://doi.org/10.1016/j.chemgeo.2008.08.009)
- Pandeli, E., Ferrini, G., Lazzari, D., 1994. Lithofacies and petrography of the Macigno Fm. from the Abetone to the Monti del Chianti areas (Northern Apennines). *Mem. Soc. Geol. Ita.* 48, 321–329.
- Perri, F., 2008. Clay mineral assemblage of the Triassic–Jurassic mudrocks from Western-Central Mediterranean Regions. *Per. Mineral.* 77, 23–40. DOI:[10.2451/2008PM0002](https://doi.org/10.2451/2008PM0002)

- Perri, F., 2014. Composition, provenance and source weathering of Mesozoic sandstones from Western-Central Mediterranean Alpine Chains. *Journal of African Earth Sciences*, 91, 32-43. DOI:10.1016/j.jafrearsci.2013.12.002
- Perri, F., Rizzo, G., Mongelli, G., Critelli, S., Perrone, V., 2008a. Zircon compositions of Lower Mesozoic redbeds of the Tethyan Margins, West-Central Mediterranean area. *International Geol. Rev.* 50, 1022–1039. DOI: 10.2747/0020-6814.50.11.1022
- Perri, F., Cirrincione, R., Critelli, S., Mazzoleni, P., Pappalardo, A., 2008b. Clay mineral assemblages and sandstone compositions of the Mesozoic Longobucco Group, northeastern Calabria: implications for burial history and diagenetic evolution. *Int. Geol. Rev.* 50, 1116–1131. DOI: 10.2747/0020-6814.50.12.1116
- Perri, F., Critelli, S., Mongelli, G., Cullers, R.L., 2011a. Sedimentary evolution of the Mesozoic continental redbeds using geochemical and mineralogical tools: the case of Upper Triassic to Lowermost Jurassic M.te di Gioiosa mudstones (Sicily, Southern Italy). *Int. J. E. Sc.* 100, 1569–1587. DOI: 10.1007/s00531-010-0602-6
- Perri, F., Muto F., Belviso, C., 2011b. Links between composition and provenance of Mesozoic siliciclastic sediments from western Calabria (southern Italy). *Ital. J. Geosci.* 130, 318-329. DOI: 10.3301/IJG.2011.04
- Perri, F., Critelli, S., Cavalcante, F., Mongelli, G., Dominici, R., Sonnino, M., De Rosa, R., 2012a. Provenance signatures for the Miocene volcanoclastic succession of the Tufiti di Tusa Fm., southern Apennines, Italy. *Geol. Magazine*, 149, 423-442. DOI:10.1017/S001675681100094X
- Perri, F., Critelli, S., Dominici, R., Muto, F., Tripodi, V., Ceramicola, S., 2012b. Provenance and accommodation pathways of late Quaternary sediments in the deep-water northern Ionian Basin, southern Italy. *Sed. Geo.* 280, 244–259. DOI:10.1016/j.sedgeo.2012.01.007

- Perri, F., Borrelli, L., Gullà, G., Critelli, S., 2014. Chemical and minero-petrographic features of Plio-Pleistocene fine-grained sediments in Calabria, southern Italy. *Ital. J. Geosci.* 133, 101-115. DOI: [10.3301/IJG.2013.17](https://doi.org/10.3301/IJG.2013.17)
- Perri, F., Ohta T., 2014. Paleoclimatic conditions and paleoweathering processes on Mesozoic continental redbeds from Western-Central Mediterranean Alpine Chains. *Palaeogeography, Palaeoclimatology, Palaeoecology*, 395, 144–157. DOI: [10.1016/j.palaeo.2013.12.029](https://doi.org/10.1016/j.palaeo.2013.12.029)
- Perri, F., Dominici, R., Critelli, S., 2015. Stratigraphy, composition and provenance of argillaceous marls from the Calcare di Base Fm., Rossano Basin (northeastern Calabria). *Geol. Magazine*, 152, 193-209. DOI:[10.1017/S0016756814000089](https://doi.org/10.1017/S0016756814000089)
- Perrone citations**
- Perrone et al. (1998) *C.R. Acad Sci* 326, 347-353;
- Perrone et al., (2008) *Boll Soc Geol It*, 127, 357-373;
- Perrone et al., (2014) *Paleo3* 394, 128-143
- Piccioni, R., Monaco, P., 1999. Caratteri sedimentologici, ichnologici e micropaleontologici delle unità eoceniche degli scisti varicolori nella sezione di M. Solare. *Boll. Serv. Geol. d'It.*, CXV, 143-188.
- Plesi, G., Luchetti, L., Boscherin, A., Botti, F., Brozzetti, F., Bucefalo Palliani, R., Daniele, G., Motti, A., Nocchi, M., Rettori, R., 2002. The Tuscan successions of the high Tiber Valley (Foglio 289 - Città di Castello): biostratigraphic, petrographic and structural features, regional correlations. *Boll. Soc. Geol. It., Vol. Spec.*, 121 (1), 425-436.
- Ricci Lucchi, F., 1986. The Oligocene to recent foreland basins of the northern Apennines. *Int. Assoc. Sedimentol. Spec. Publ.* 8, 105–139.
- Ricci Lucchi, F., 1990. Turbidites in foreland and on-thrust basins of the northern Apennines. *Palaeogeogr Palaeoclimatol Palaeoecol*, 77: 51–66. DOI: [10.1016/0031-0182\(90\)90098-R](https://doi.org/10.1016/0031-0182(90)90098-R)

- Ricci Lucchi, F., Valmori, E., 1980. Basin-wide turbidites in a Miocene, oversupplied deep-sea plain: a geometrical analysis. *Sedimentology*, 27, 241-270. DOI: [10.1111/j.1365-3091.1980.tb01177.x](https://doi.org/10.1111/j.1365-3091.1980.tb01177.x)
- Roy, P.D., Caballero, M., Lozano, R., Smytatz-Kloss, W., 2008. Geochemistry of late quaternary sediments from Tecomuco lake, central Mexico: Implication to chemical weathering and provenance. *Chemie der Erde*, 68, 383-393. DOI: [10.1016/j.chemer.2008.04.001](https://doi.org/10.1016/j.chemer.2008.04.001)
- Sames, C.W., 1966. Morphometric data of some recent pebble associations and their applications to ancient deposits. *J. Sed. Petr.* 36, 126–142.
- Schneider, R.R., Price, B., Muller, P.J., Kroon, D., Alexander, I., 1997. Monsoon-related variations in Zaire (Congo) sediment load and influence of fluvial silicate supply on marine productivity in the east equatorial Atlantic during the last 200,000 years. *Paleoceanography*, 12, 463-481. DOI: [10.1029/96PA03640](https://doi.org/10.1029/96PA03640)
- Shanmugan, G., 2002. Ten turbidite myths. *Earth-Sci. Rev.*, 58, 311-341. DOI: [10.1016/S0012-8252\(02\)00065-X](https://doi.org/10.1016/S0012-8252(02)00065-X)
- Suttner, L.J., 1974. Sedimentary petrographic province: an evaluation. *Society of Economic Paleontologists and Mineralogists Special Publication* 21, 75–84.
- Talling, P.J., Amy, L.A., Wynn, R.B., Peakall, J., Robinson, M., 2004. Beds comprising debrite sandwiched within co-genetic turbidite: origin and widespread occurrence in distal depositional environments. *Sedimentology*, 51, 163-194. DOI: [10.1111/j.1365-3091.2004.00617.x](https://doi.org/10.1111/j.1365-3091.2004.00617.x)
- Taylor, S.R., McLennan, S.M., 1985. *The continental crust: its composition and evolution*. Blackwell, Oxford.
- Tinterri, R., Muzzi Magalhaes, P., 2011. Synsedimentary structural control on foredeep turbidites: An example from Miocene Marnoso-arenacea Fm., Northern Apennines, Italy. *Mar. Petrol. Geol.* 28, 629-657. DOI: [10.1016/j.marpetgeo.2010.07.007](https://doi.org/10.1016/j.marpetgeo.2010.07.007)

- Trecci, T., Monaco, P., 2011. Le ichnocenosi delle successioni sedimentarie Eocenico-Mioceniche affioranti tra il Lago Trasimeno e l'Alpe di Poti (Appennino Settentrionale). *Annali di Ferrara, Museol. Scient. Natural.*, 7, 1-101.
- Trincardi, F., Verdicchio, G., Asioli, A., 2005. Comparing Adriatic contourite deposits and other Mediterranean examples. In: F.I.S.T. (Ed.), *GeoItalia 2005, Spoleto 21-23 Settembre 2005*, 321 pp.
- Valloni, R., Lazzari, D., Calzolari, M. A., 1991. Selective alteration of arkose framework in Oligo-Miocene turbidites of the Northern Apennines foreland: impact on sedimentary provenance analysis. From Morton, A. C., Todd, S. P., Haughton, P. D. W. (eds) 1991, *Developments in Sedimentary Provenance Studies. GSA Special Publication, No 57*, 125-136. DOI: [10.1144/GSL.SP.1991.057.01.11](https://doi.org/10.1144/GSL.SP.1991.057.01.11)
- Van de Kamp, P.C., Leake, B.E., 1985. Petrography and Geochemistry of Feldspathic and Mafic Sediments of the Northeastern Pacific Margin. *Transactions of the Royal Society of Edinburgh: Earth Sciences*, 76, 411-449.
- Van der Meulen, M.J., Meulenkamp, J.E., and Wortel, M.J.R., 1998. Lateral shifts of Apenninic foredeep depocentres reflecting detachment of subducted lithosphere. *EPSL* 154, 203–219. DOI: [10.1016/S0012-821X\(97\)00166-0](https://doi.org/10.1016/S0012-821X(97)00166-0)
- Walker, R.G. 1975. Generalized facies model for resedimented conglomerates of turbidite association. *Bull. Geol. Soc. Am.* 86: 737–748. DOI: [10.1130/0016-7606\(1975\)86<737:GFMFRC>2.0.CO;2](https://doi.org/10.1130/0016-7606(1975)86<737:GFMFRC>2.0.CO;2)
- Weaver, C.E., 1989. *Clays, muds, and shales. Developments in sedimentology*, 44. Elsevier, Amsterdam, 819 pp. ISBN 0-444-87381-3
- Wrafter, J.P., Graham, J.R., 1989. Ophiolitic detritus in the Ordovician sediments of South Mayo Ireland. *J. Geol. Soc. London* 146, 213–215. DOI: [10.1144/gsjgs.146.2.0213](https://doi.org/10.1144/gsjgs.146.2.0213)

- Wronkiewicz, D.J., Condie, K.C., 1989. Geochemistry and provenance of sediments from the Pongola Supergroup, South Africa: Evidence for a 3.0 Ga old continental craton. *Geoch. Cosmochim. Acta*, 53, 1537-1549. DOI: [10.1016/0016-7037\(89\)90236-6](https://doi.org/10.1016/0016-7037(89)90236-6)
- Wronkiewicz, D.J., Condie, K.C., 1990. Geochemistry and mineralogy of sediments from the Ventersdorp and Transvaal Supergroup, South Africa: cratonic evolution during the early Proterozoic. *Geochim. Cosmochim. Acta*, 54, 343-354. DOI: [10.1016/0016-7037\(89\)90236-6](https://doi.org/10.1016/0016-7037(89)90236-6)
- Zaghloul, M.N., Critelli, S., Perri, F., Mongelli, G., Perrone, V., Sonnino, M., Tucker, M., Aiello, M., Ventimiglia, C., 2010. Depositional systems, composition and geochemistry of Triassic rifted continental margin redbeds of Internal Rif Chain, Morocco. *Sedimentology* 57, 312–350. DOI: [10.1111/j.1365-3091.2009.01080.x](https://doi.org/10.1111/j.1365-3091.2009.01080.x)
- Zuffa, G.G., 1980. Hybrid arenites: their composition and classification. *Journ. of Sed. Petrol.*, 50, 21-29. DOI: [10.1306/212F7950-2B24-11D7-8648000102C1865D](https://doi.org/10.1306/212F7950-2B24-11D7-8648000102C1865D)
- Zuffa, G.G., 1985. Optical analyses of arenites: influence of methodology on compositional results. In: Zuffa, G.G. (Ed.), *Provenance of Arenites*. Dordrecht, The Netherlands, NATO Advanced Study Institute Series, Reidel, 148, pp. 165–189. DOI: [10.1007/978-94-017-2809-6_8](https://doi.org/10.1007/978-94-017-2809-6_8)
- Zuffa, G.G., 1987, Unravelling hinterland and offshore palaeo- geography from deep-water arenites: in Leggett, J.K. and Zuffa, G.G., eds., *Marine Clastic Sedimentology, models and case studies*, Graham and Trotman, London, p. 39-61. DOI: [10.1007/978-94-009-3241-8_2](https://doi.org/10.1007/978-94-009-3241-8_2)

Figure captions

Fig. 1. Outcrop distribution of main Northern Apennines turbidite foredeep units, with indication of study area (modified after [Dunkl et al., 2001](#)).

Fig. 2. Synthetic geological map of the Trasimeno Lake area showing outcrops of the Tuscan and Umbria successions and location of sections (after [Monaco and Trecci, 2014](#)).

Fig. 3. Schematic synthetic stratigraphic columns of the Poggio Belvedere Member (MAC2), with the lithology and location of studied samples.

Fig. 4. Outcrops of the Poggio Belvedere Member in Trasimeno Lake area. (A) General view of the upper Pianello section deposits showing alternation between thin-bedded fine-grained turbidites (F9b facies of Mutti, 1992) and massive coarse-grained sandstones (F5-F7 facies of [Mutti, 1992](#)). (B) Detail of multidirectional lineations in sandy horizons in the uppermost portion of the Pianello Stratigraphic section (red lines indicate direction of palaeocurrents). (C) View of massive sandy horizons (F6 facies) including West-oriented flute casts in the upper Pianello Stratigraphic section. (D) View of mid-lower Renali section deposits, with presence of basal calcirudite and calcarenite levels (among yellow lines) interfingering within deep-water siliciclastic succession. (E) Alternating mudstones and fine-grained sandstones interfingering with thin massive coarse-grained sandy horizon at Maestà Stratigraphic section. (F) Detail of convolute laminations of a sandy level within fine-grained turbidite deposits (T_c of Bouma sequence) in the Maestà Stratigraphic section.

Fig. 5. Peculiar fossil traces in studied sections. Renali Stratigraphic section (A-B): (A) The graphoglyptid *Helminthorhapse* (Hm) at sole of turbidite with other undetermined curved specimens (arrows), bar = 3 cm; (B) The graphoglyptid *Cosmorhapse isp.* at sole of turbidite, bar = 3 cm. Maestà Stratigraphic section (C-G): (C) a sole of thin turbidite with *Spirophycus* (centre) and *Spirorhapse* (arrows), scale = 10 cm; (D) a detail of *Spirophycus* (Sp) and *Spirorhapse* (Sr), bar =

10 cm; (E) a further detail on *Spirophycus bicornis* (Sp) and *Spirorhappe* (Sr) with two *Paleodictyon minimum* specimens (Pm, arrows), bar = 5; (F) the hypichnial graphoglyptid *Urohelminthoida dertonensis* at sole of turbidite, bar = 5 cm; (G) Endichnial *Halopoa* (Ha, variation *Fucusopsis*) at sole of turbidite, bar = 10 cm;

Fig. 6. Qm–F–Lt, Lm–Lv–Ls, Rg–Rs–Rm Qt–F–L and Qm–K–P triangular plots (from Dickinson, 1970; Ingersoll and Suczek, 1979; Critelli and Le Pera, 1994; Folk, 1968; Graham et al., 1976) for Poggio Belvedere sandstones of the Macigno Fm.. Qm (monocrystalline quartz), F (feldspars) and Lt (total lithic fragments); Lm (metamorphic), Lv (volcanic) and Ls (sedimentary) lithic fragments; Rg (plutonic rock fragments), Rv (volcanic rock fragments) and Rm (metamorphic rock fragments); Qt (quartz grains), F (feldspars) and L (aphanitic lithic fragments); Qm (monocrystalline quartz), K (K-feldspar) and P (plagioclase).

Fig. 7. Peculiar granular components in sandstones (crossed nicols view), bar = 500 μ m. (A) Plagioclase displaying typical albite polysynthetic twinning (*P*) and K-feldspar grains (*K*) locally replaced by calcite cement. (B) Fine-grained schist (*red arrow*) with internal muscovite and quartz grains. (C) Volcanic rock fragment with felsic granular fabric (*red arrow*) including internal plagioclase (*P*) and quartz (*Q*) phenocrysts. (D) Plutonic rock fragment with quartz (*Q*) and plagioclase crystals (*P*). (E) Metamorphic rock fragment with isoriented strips of quartz (*Q*) and K-feldspar (*K*). (F) Polycrystalline quartz grain with tectonic fabric (*Qp*). (G) Volcanic rock fragment with microlithic fabric (*red arrow*) containing phenocrysts of plagioclase (*P*) and quartz (*Q*) in a fine-grained groundmass rich in K. (H) Packstone with macroforaminifers (lepidocyclinids and nummulitids).

Fig. 8. Comparisons of studied data with previous works using Qm–F–Lt and Lm–Lv–Ls diagram plots (from Dickinson, 1970; Ingersoll and Suczek, 1979). Qm (monocrystalline quartz), F

(feldspars) and Lt (total lithic fragments); Lm (metamorphic), Lv (volcanic) and Ls (sedimentary) lithic fragments.

Fig. 9. Classification diagram for the studied mudstone samples (Herron, 1988).

Fig. 10. Normalization of major and trace elements to the upper continental crust (UCC; McLennan et al., 2006). The plot of the Post-Archean Australian Shales (PAAS; Taylor and McLennan 1985) is shown for comparison.

Fig. 11. Ternary plot showing the relative proportions of SiO₂ (representing quartz), Al₂O₃ (representing mica/clay minerals), and CaO (representing carbonate) for the studied mudstone samples.

Fig. 12. Palaeogeographic and geodynamic model of the central-western Mediterranean area showing the possible source areas for Macigno foredeep system (modified after Guerrera et al., 2015).

Fig. 13. Provenance diagram based on the Cr/V vs. Y/Ni relationships (after Hiscott 1984). Curve model mixing between felsic and ultramafic end-members.

Fig. 14. V-Ni-La*10 ternary diagram, showing fields representative of felsic, mafic and ultramafic rocks plot separately (e.g., Bracciali et al., 2007; Perri et al., 2011b).

Fig. 15. Ternary (A) A–CN–K (Nesbitt and Young, 1982) and (B) A–C–N (Perri et al., 2014, 2015) plots. Key: A, Al₂O₃; C, CaO; N, Na₂O; K, K₂O; Gr, granite; Ms, muscovite; Ill, illite; Kln, kaolinite; Chl, chlorite; Gbs, gibbsite; Smt, smectite; Plg, plagioclase; Kfs, K-feldspar; Bt, biotite; Ab, albite.

Fig. 16. Ternary 15*Al₂O₃–300*TiO₂–Zr plot after García et al. (1994) for the studied mudstone samples.

Table caption

Table 1. Sandstone raw data. Categories used for sandstone samples point counts and assigned grains in recalculated plots are those of [Zuffa \(1985, 1987\)](#), [Critelli and Le Pera \(1994\)](#), and [Critelli and Ingersoll \(1995\)](#). R.f.=coarse grained rock fragments; NCE=noncarbonate extrabasinal grains; CI=carbonate intrabasinal grains.

Tables 2. Recalculated modal point count data.

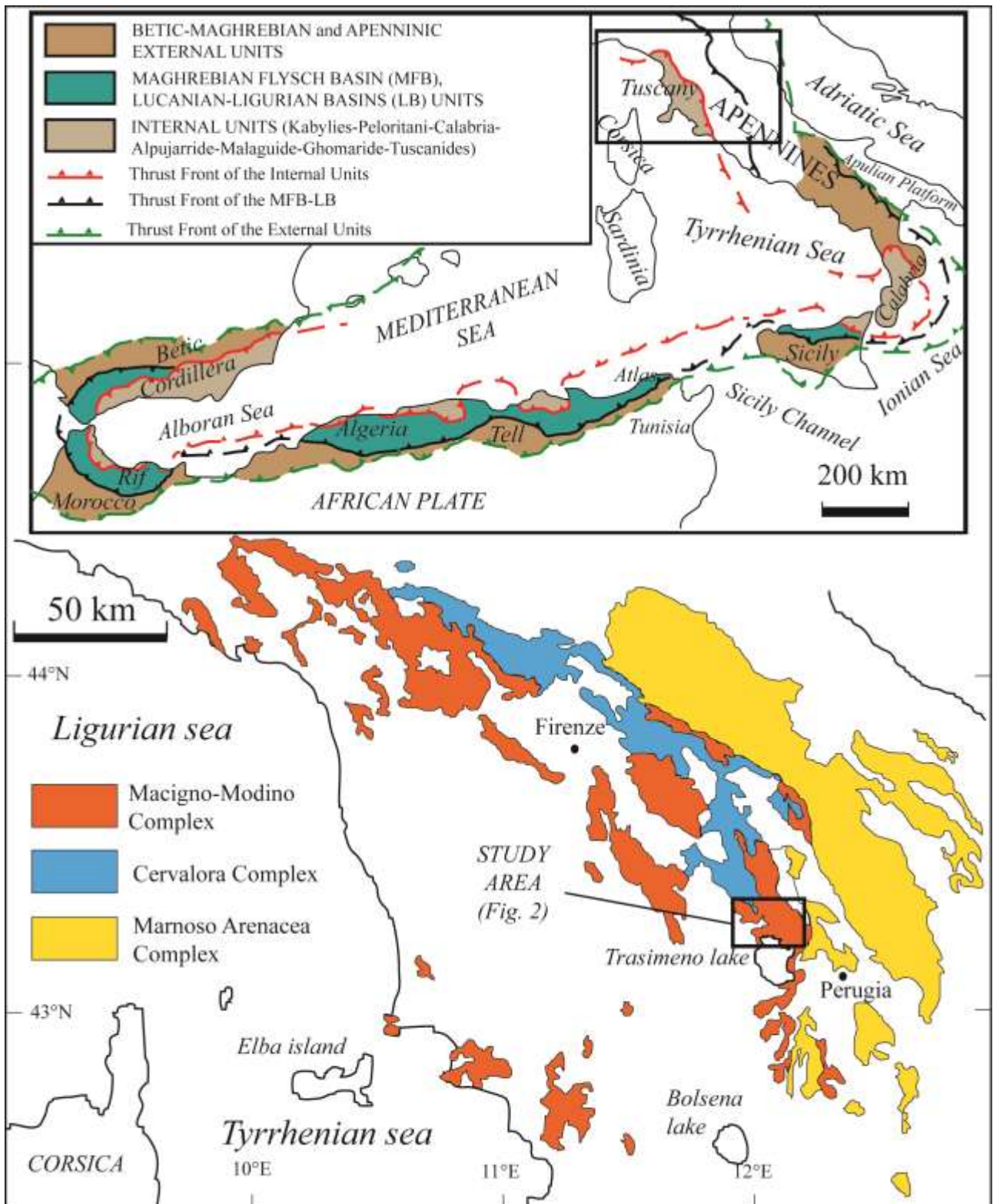
Note: X=mean, s.d= standard deviation. Qm=monocrystalline quartz, Qp=polycrystalline quartz, F=feldspars (K+P), K=K-feldspar, P=plagioclase; Lt=lithic grains; Lm=metamorphic, Lv=volcanic, and Ls=sedimentary lithic grains; Lvm=volcanic and metavolcanic, Lsm=sedimentary and metasedimentary lithic grains; Rg=phaneritic plutonic rock fragments; Rm=coarse and fine grained metamorphic rock fragments; Rv=coarse and fine grained volcanic rock fragments; Rs=coarse and fine grained sedimentary rock fragments.

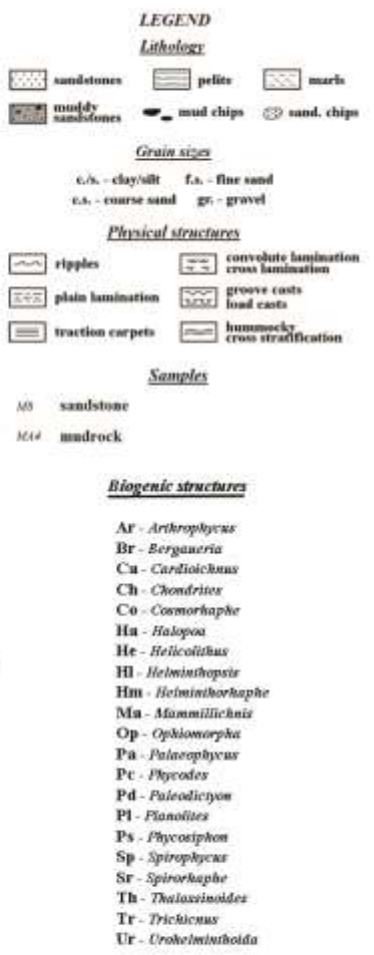
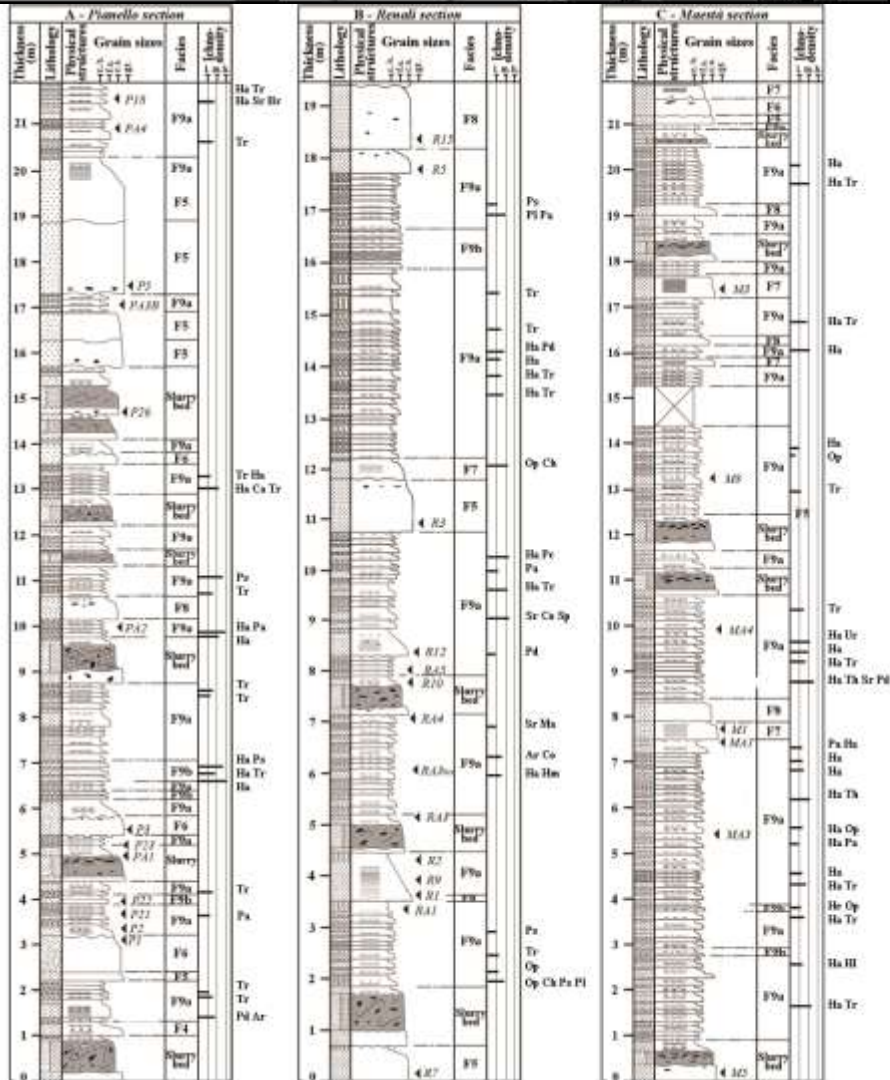
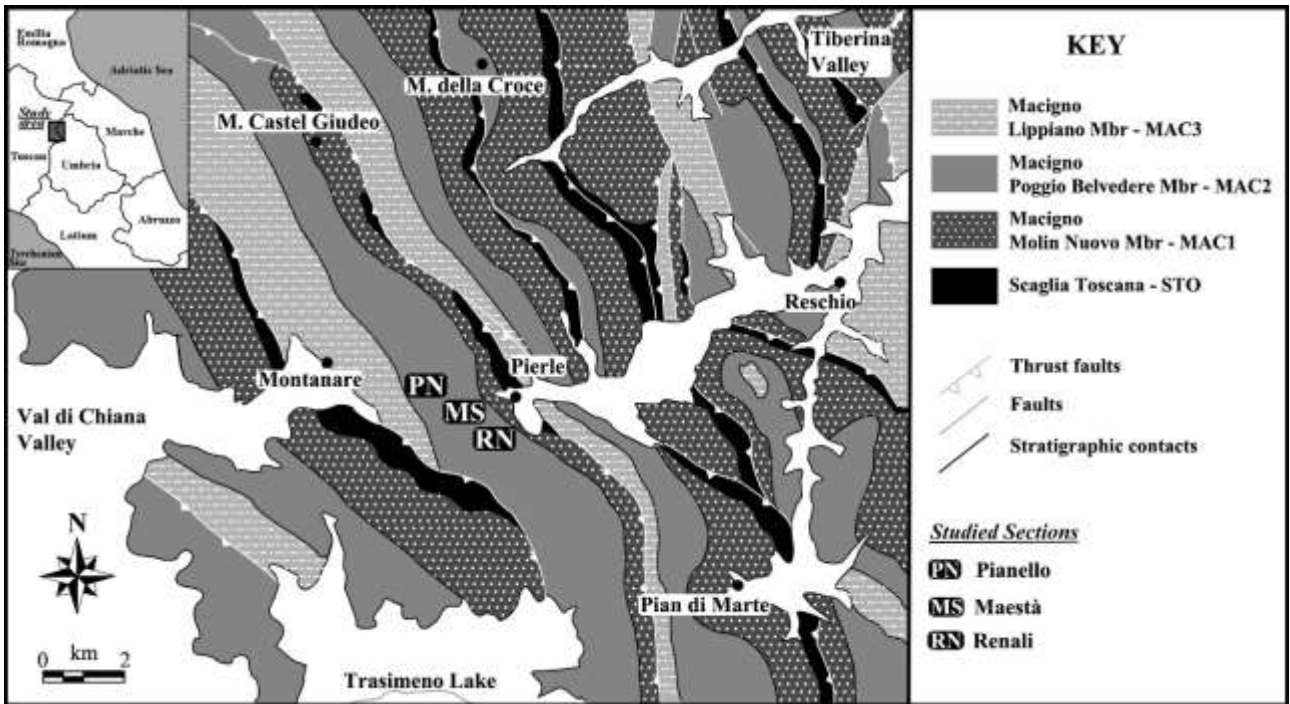
Table 3. Average petrological parameters and ratios of Poggio Belvedere sandstones compared with Macigno sandstones and Calabrian arc sands (after [Ibbeken and Schleyer, 1991](#); [Perri et al., 2012b](#)); standard deviation in brackets.

Note: *Data reported after [Ibbeken and Schleyer, 1991](#); ** Data reported after [Perri et al., 2012b](#).

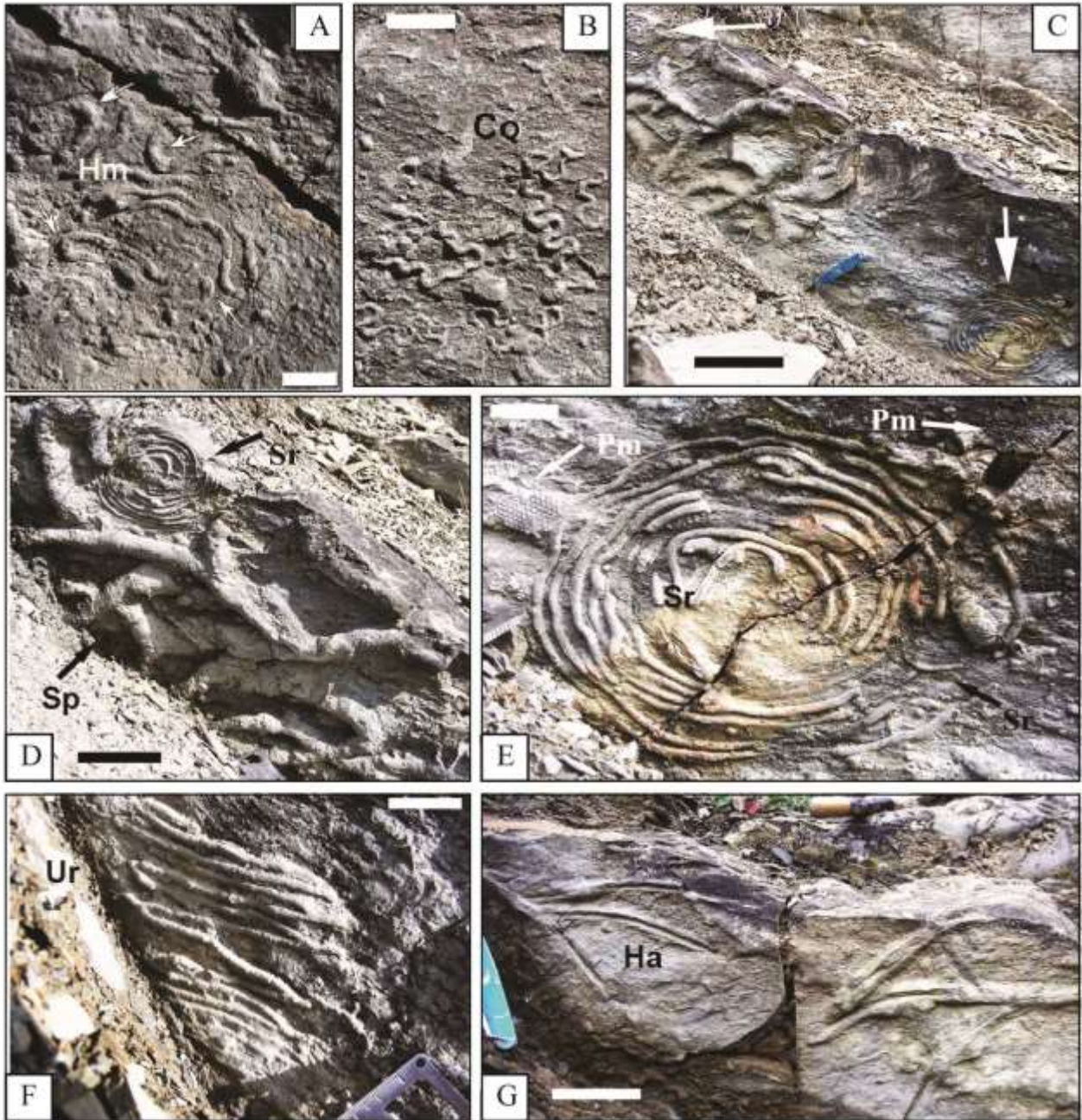
Table 4. Mineralogical composition of the bulk rock (weight percent).

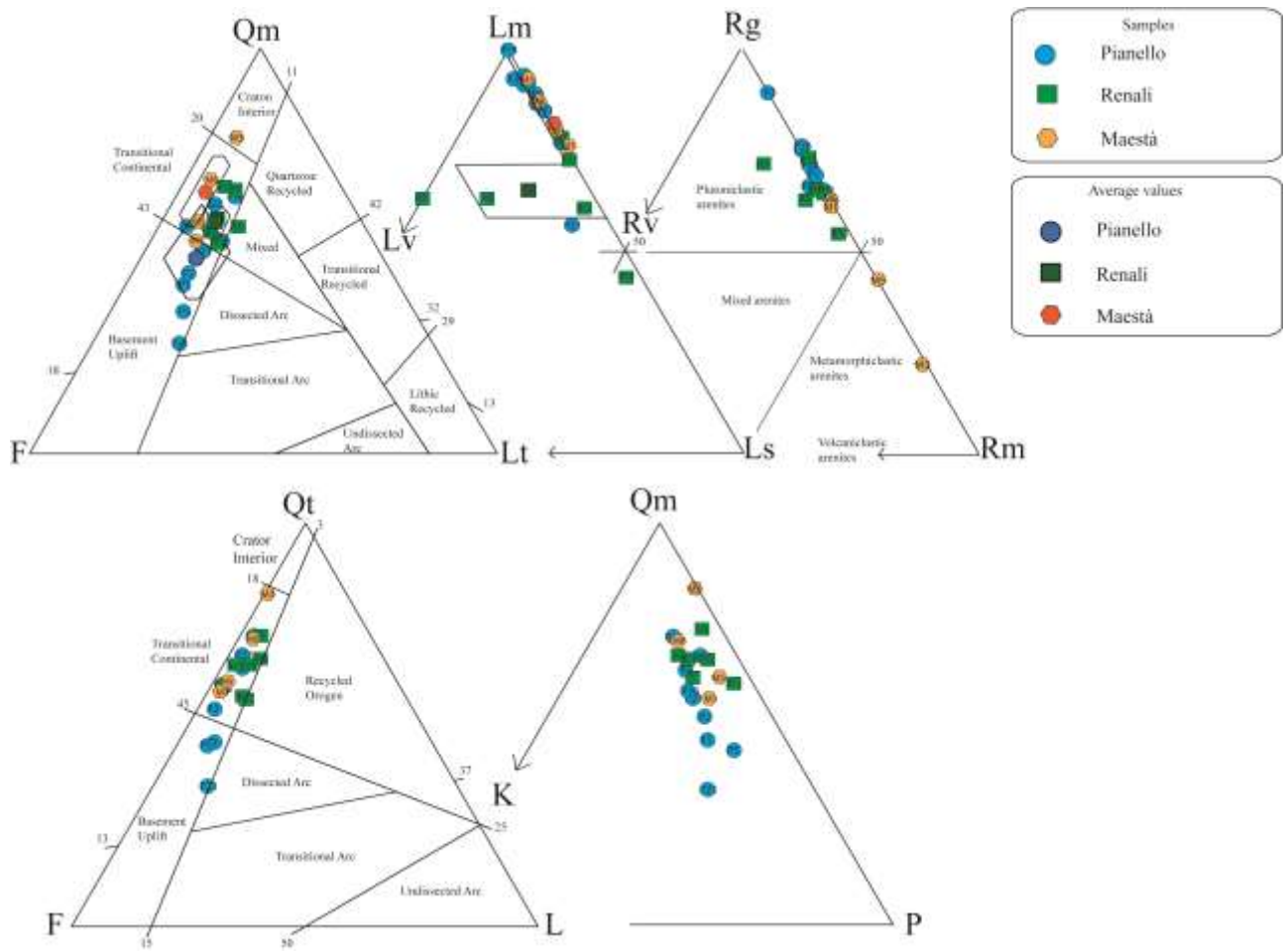
Table 5. Major, trace element and ratios distribution of mudstone samples.

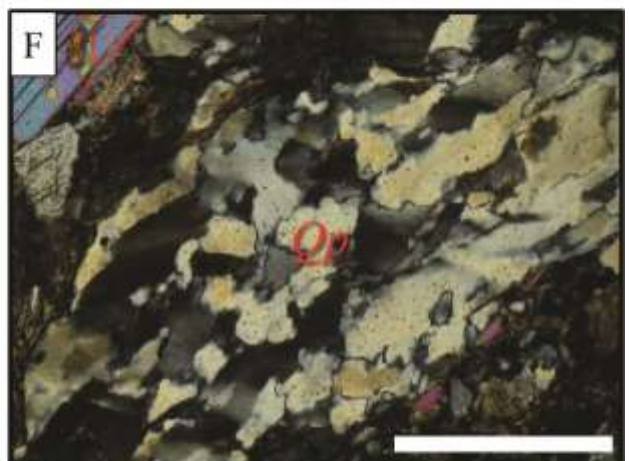
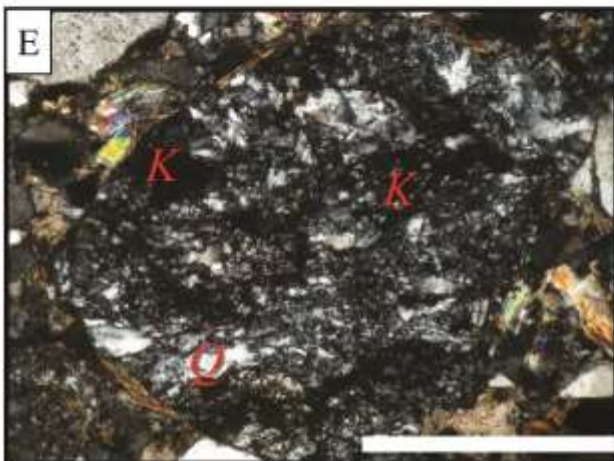
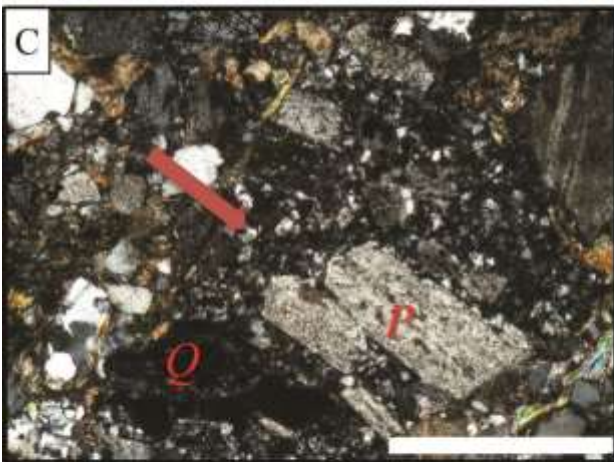
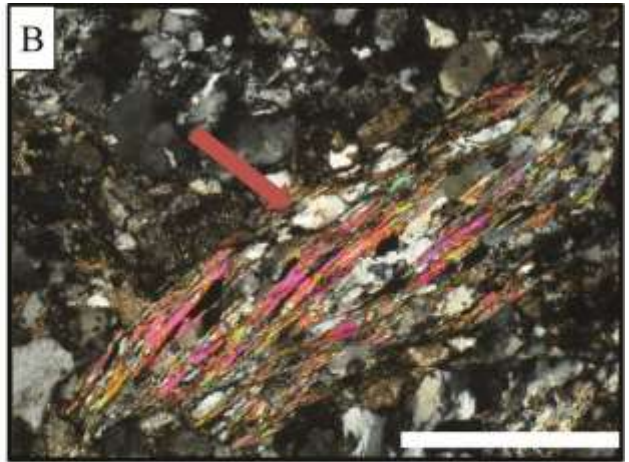
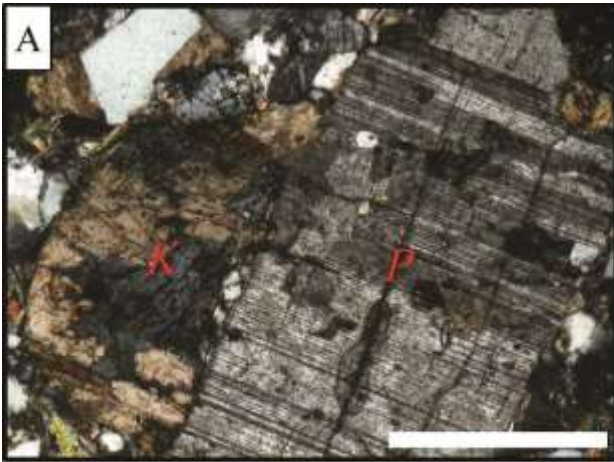


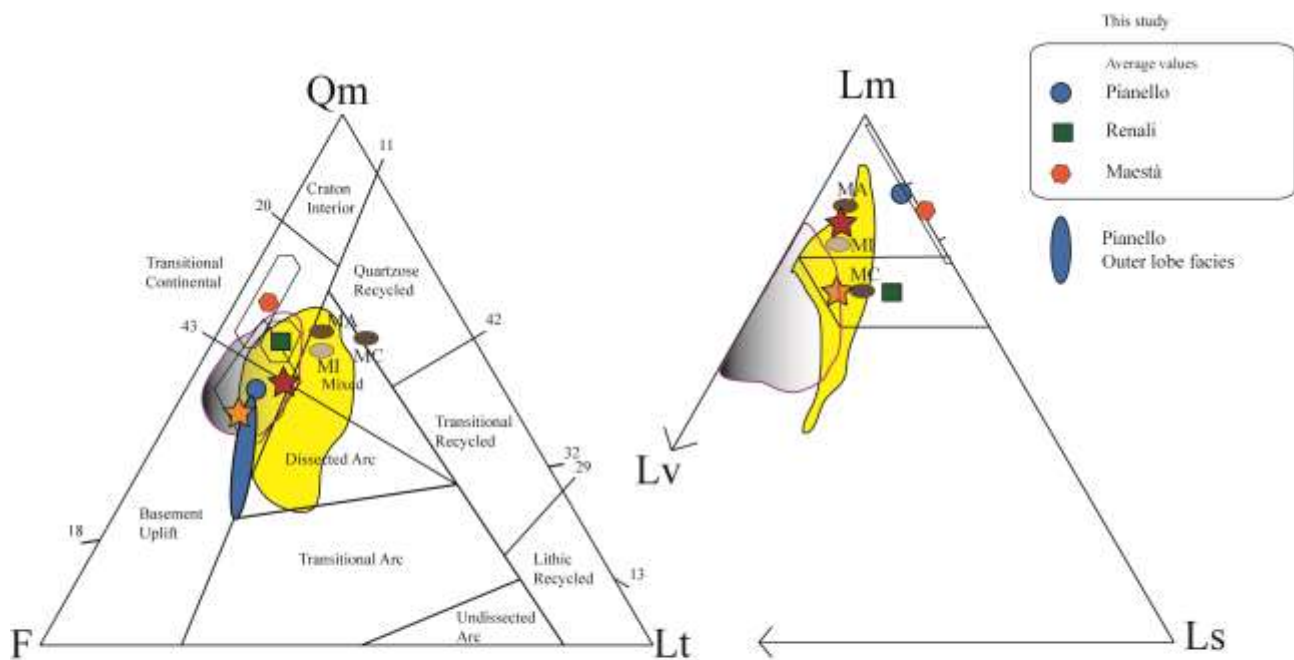












Data from Valloni et alii, 1991

Macigno Fm. of NW Tuscany

Data from Cornamusini, 2002

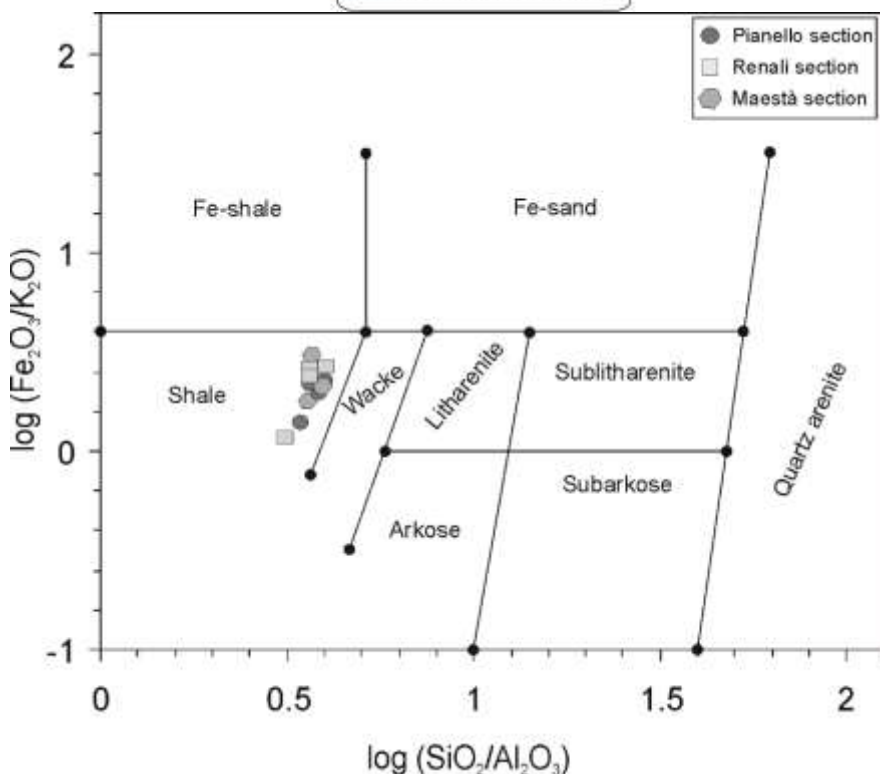
Average values:
 Macigno Costiero (MC)
 Macigno Intermedio (MI)
 Macigno Appenninico (MA)

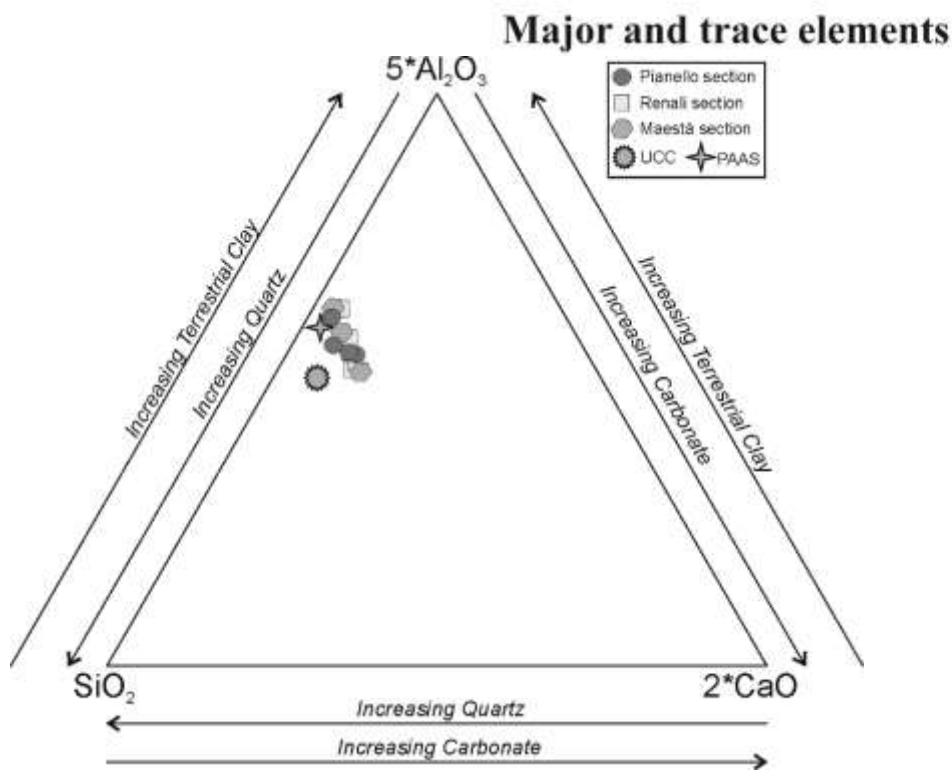
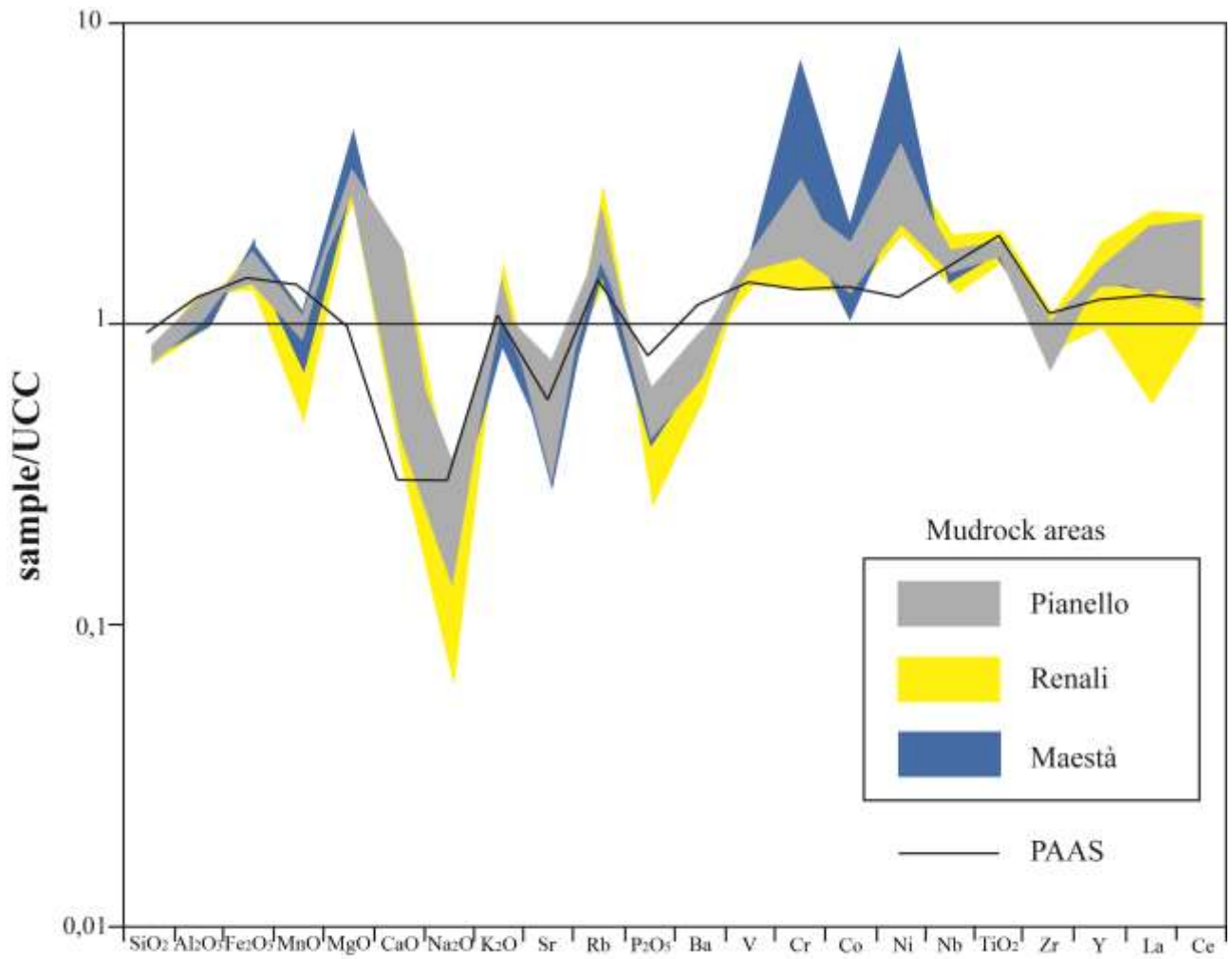
Data from Bruni et alii, 2007

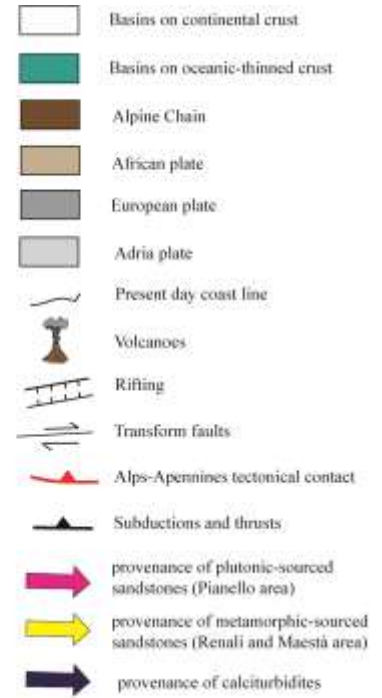
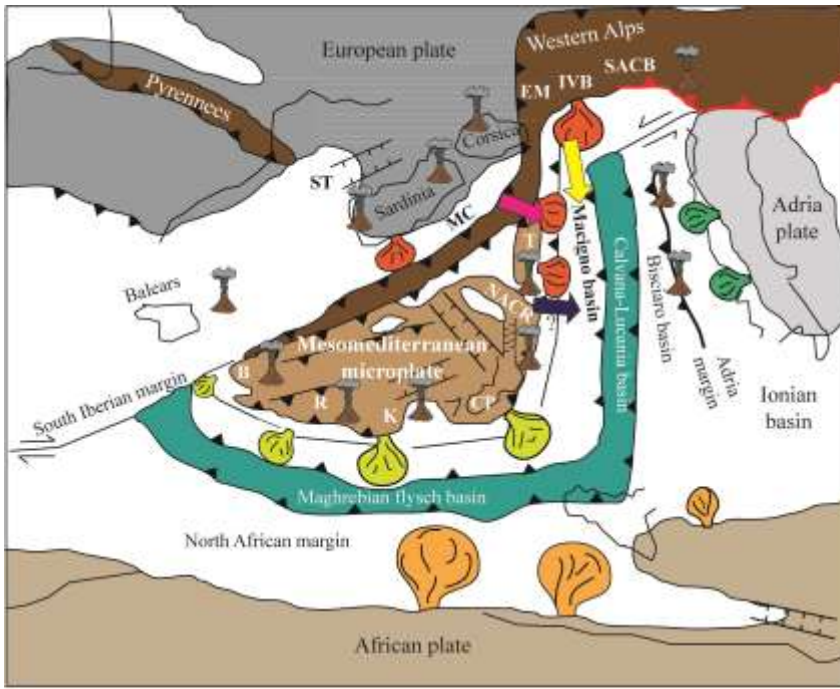
Macigno Fm. Abetone area Average value
 GO 24 sample

Data from Barsella et alii, 2009

Macigno P. Belvedere Member

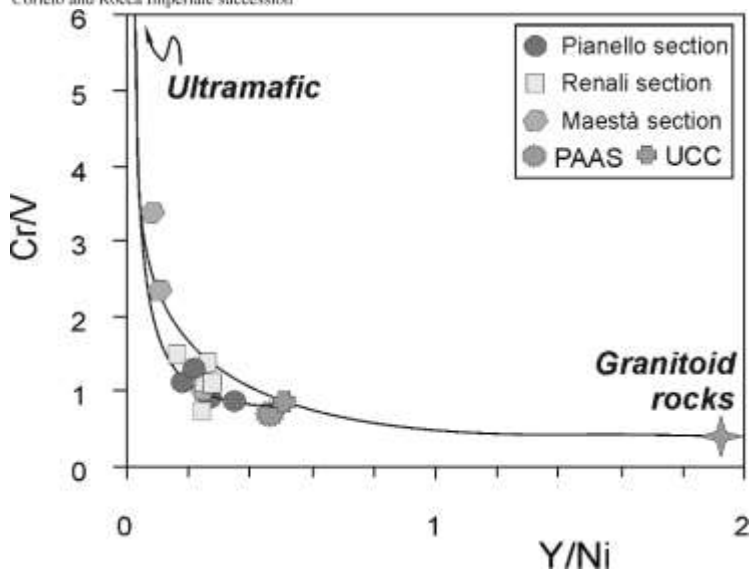


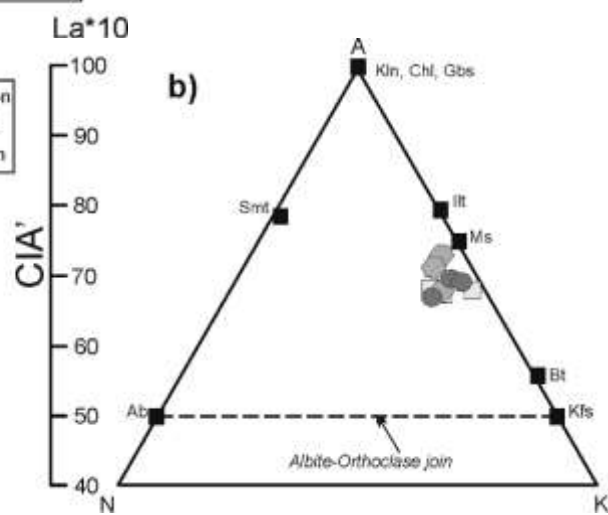
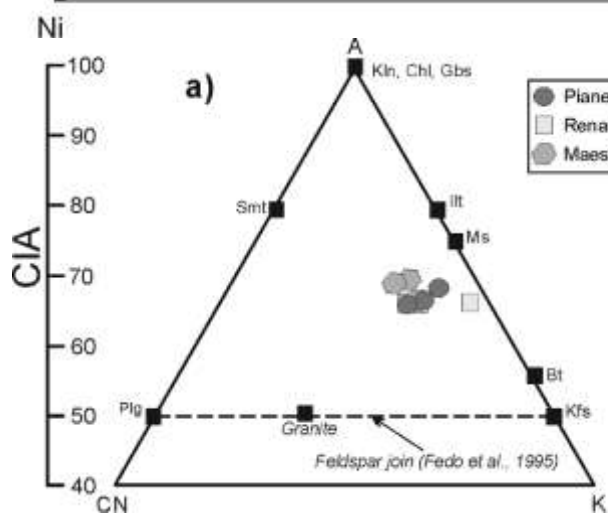
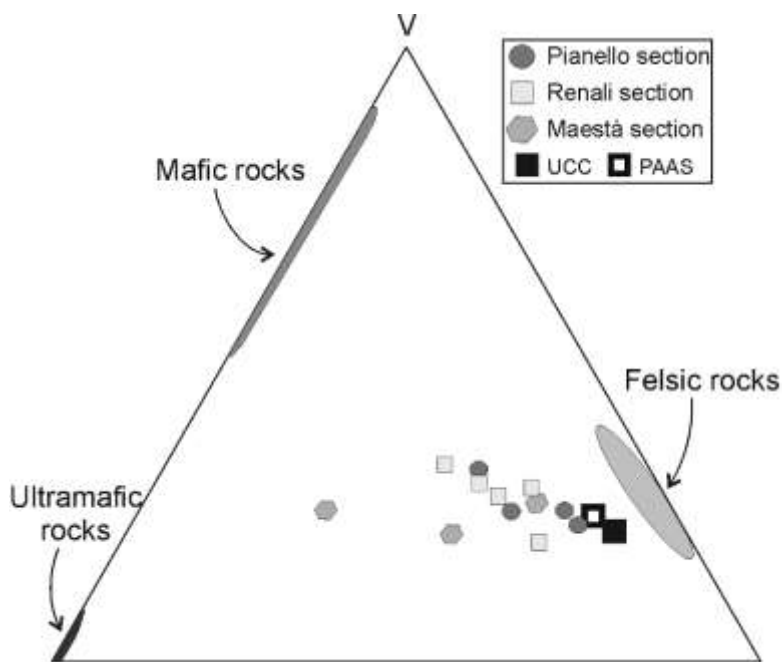


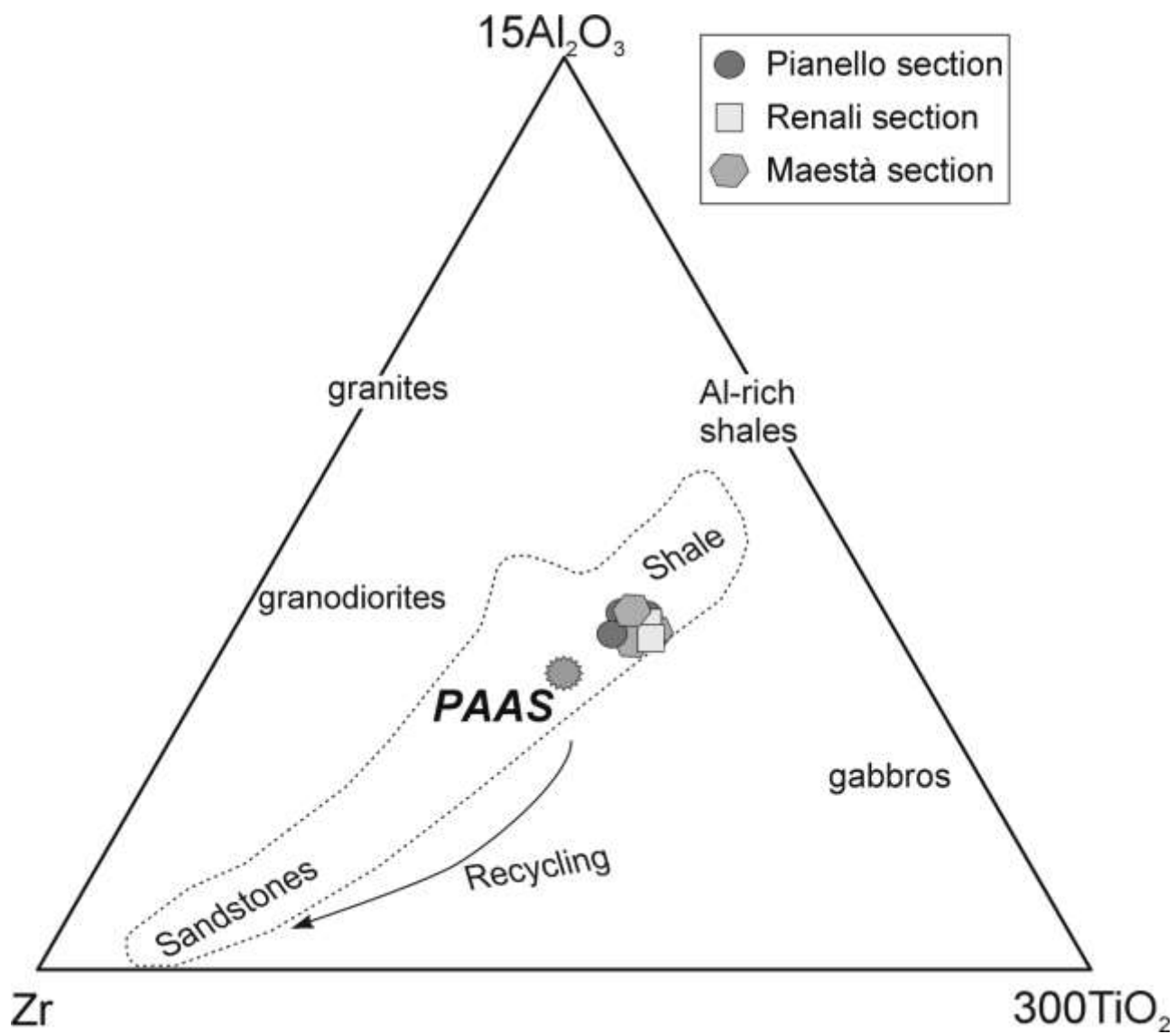


ST: Sardinia trough
B: Betic succession
R: Rifian succession
K: Kabylia succession
CP: Calabria-Peloritani succession
NACR: North Calabria, Albanella, Corleto and Rocca Imperiale succession
T: Internal Tuscanide succession
MC: Macigno Costiero Fm.
EM: External massifs
IVB: Ivrea-Verbano Block
SACB: South Alpine Crystalline Basement

Numidian fan delta (Qtzarenitic composition)
 Macigno fan delta (Qtzfeldspathic composition)
 Internal flysch fan delta (Qtzlitic composition)
 Adria fan delta (Carbonate composition)







		Poggio Belvedere member																		
		Pianello area								Renali area						Maestà area				
		outer lobe facies				fringe-basin facies				sl. div.	out. lobe		basin		slur. Div.		out. Lobe		Bas.	s.d.
		P1	P23	P3	P5	P2	P21	P22	P18	P26	R7	R3	R12	R5	R10	R15	M1	M3	M8	M5
NCE	Q																			
	Quartz (single crystals)	85	39	89	54	65	90	112	85	121	87	124	89	103	116	118	105	183	142	133
	Polycrystalline quartz with tectonic fabric	6	9	17	19	14	13	12	12	5	6	10	12	7	11	7	8	6	4	4
	Polycrystalline quartz without tectonic fabric	11	8	19	10	11	12	9	16	4	4	10	5	6	13	5	3	0	4	2
	Quartz in metamorphic r.f.	3	0	4	7	1	4	2	3	0	1	3	1	7	2	1	1	0	0	2
	Quartz in plutonic r.f.	20	25	27	33	32	28	26	22	17	37	24	19	23	14	13	9	1	2	4
	Quartz in plutonic or gneissic r.f.	3	1	11	2	3	1	8	2	0	6	1	2	4	0	3	1	1	0	0
	Quartz in sandstone	0	1	0	0	0	0	0	0	0	0	0	0	0	0	0	0	0	0	0
	Calcite replacement on Quartz	7	7	15	4	20	12	17	59	22	15	28	31	17	20	27	17	6	25	1
	K																			
	K-feldspar (single crystals)	33	29	17	8	32	27	11	17	30	24	10	11	22	14	21	21	3	19	17
	K-feldspar in metamorphic r.f.	0	1	2	1	0	1	7	1	0	0	0	0	0	0	0	0	0	0	1
	K-feldspar in plutonic r.f.	10	17	9	11	4	6	0	5	5	6	3	1	5	3	2	3	0	3	0
	K-feldspar in plutonic or gneissic r.f.	0	1	2	0	1	1	0	0	0	2	0	0	0	0	1	1	0	0	0
	K-feldspar in sandstone	0	0	0	0	0	0	0	0	0	0	1	0	0	0	0	0	0	0	0
	Calcite replacement on K-feldspar	2	2	3	9	3	1	4	4	10	1	0	0	0	1	3	1	0	5	0
	P																			
	Plagioclase (single crystals)	59	53	36	35	34	39	32	27	51	35	43	58	35	35	45	55	37	34	65
	Plagioclase in metamorphic r.f.	1	4	0	5	0	0	1	0	0	0	0	1	1	1	0	0	0	0	0
	Plagioclase in plutonic r.f.	14	20	14	45	20	20	17	4	3	21	7	9	12	5	10	8	0	4	4
	Plagioclase in plutonic or gneissic r.f.	2	3	1	3	2	0	0	1	0	0	0	4	1	1	0	1	0	0	1
	Plagioclase in sandstone	0	1	0	0	0	0	0	0	0	0	0	0	0	0	0	0	0	0	0
	Calcite replacement on Plagioclase	16	12	5	19	20	9	9	12	12	5	3	9	1	16	7	11	0	5	0
	M																			
	Micas and chlorite (single crystals)	21	16	12	25	27	24	34	35	28	34	19	23	41	29	37	50	67	49	69
	Micas and chlorite in plutonic r.f.	4	3	3	1	4	3	11	5	0	3	1	0	3	2	0	0	0	0	0
	Micas and chlorite in metamorphic r.f.	2	1	0	1	0	0	1	0	0	2	0	0	2	0	0	0	0	0	0
	Micas and chlorite in plutonic or gneissic r.f.	0	1	1	0	0	3	0	0	0	0	1	2	2	0	0	0	0	1	1
	L																			
	Volcanic lithic with felsic granular texture	0	4	1	0	0	0	0	0	0	1	0	0	0	0	0	0	0	0	0
	Volcanic lithic with microlithic texture	0	0	0	0	0	0	0	0	0	2	0	0	2	1	0	0	0	0	0
	Other volcanic lithic	0	0	0	0	0	0	0	0	0	7	0	1	3	0	0	0	0	0	0
	Phyllite	5	3	6	6	4	2	0	3	0	3	3	1	2	1	0	0	0	1	0
	Fine grained schists	3	5	3	2	1	0	1	2	2	5	0	4	2	3	2	3	1	1	2
	Impure chert	1	2	2	2	0	2	0	0	1	0	2	2	0	1	0	5	2	1	0
	Sedimentary lithic	0	13	0	1	2	1	3	0	0	0	3	11	3	9	3	0	0	0	1
	Slate	3	4	1	1	1	1	1	1	1	2	4	2	1	1	0	0	0	0	1
	Chlorite/Muscovite schist	0	3	0	1	0	0	0	0	0	0	0	2	2	1	1	3	0	0	4
CE	Bioclasts	0	0	0	0	0	0	0	0	0	0	0	0	0	12	1	0	0	0	0
Mx	Siliciclastic matrix	46	30	56	4	41	54	33	1	40	24	28	31	49	79	3	28	2	12	30
	Epi matrix	1	0	2	3	2	1	3	1	0	0	0	0	0	1	4	1	3	3	0
	Pseudomatrix	0	0	0	6	17	4	1	3	0	1	1	2	2	0	1	4	6	3	7
Cm	Carbonate cement (pore-filling)	0	4	0	1	0	4	0	68	2	0	0	0	0	2	0	0	0	2	0
	Carbonate cement (patchy-calcite)	0	0	0	2	0	2	0	0	6	2	2	4	2	4	0	0	0	1	0
	Calcite replacement on undetermined grains	0	4	2	2	0	2	2	3	2	3	1	1	4	4	0	0	0	1	0
	Quartz overgrowth	0	1	0	0	0	0	0	0	0	0	0	0	0	0	0	0	0	0	0
	Undetermined grains																			
TOT		358	327	360	323	361	367	357	392	362	339	332	338	364	400	317	339	318	322	349

Section	Facies	Sample	% Qm			% F			% Lt			% Qt			% F			% L			% Qm			% K			% P			% Qp			% Lvm			% Lsm			% Lm			% Lv			% Ls			% Rg			% Rv			% Rm			% Rg			% Rs			% Rm			index			
			Qm	F	Lt	Qt	F	L	Qm	K	P	Qp	Lvm	Lsm	Lm	Lv	Ls	Rg	Rv	Rm	Rg	Rs	Rm	Lv/L	P/F	Q/F	F/L																																										
Maestà area	slurried div.	M5	58	36	6	60	37	3	61	8	31	43	0	57	92	0	8	42	0	58	40	4	56	0	0,79	1,59	6,29																																										
	basin plain	M8	68	28	4	71	28	1	70	12	18	82	0	18	86	0	14	63	0	37	59	6	35	0	0,61	2,41	6,36																																										
	outer lobe	M3	79	17	4	83	16	1	83	1	16	89	0	11	78	0	22	22	0	78	18	18	64	0	0,92	4,77	4,44																																										
	outer lobe	M1	52	39	9	58	39	3	57	11	32	73	0	27	74	0	26	61	0	39	53	12	35	0	0,74	1,32	4,59																																										
		outer lobe		66	28	6	71	27	2	70	6	24	81	0	19	76	0	24	42	0	58	36	15	49	0	0,83	3,05	4,52																																									
		X		64	30	6	68	30	2	68	8	24	72	0	28	82	0	18	47	0	53	43	10	48	0	0,8	2,5	5,4																																									
	s.d.		12	10	2	12	10	1	12	5	8	20	0	20	8	0	8	19	0	19	18	6	15																																														
Renali area	slurried div.	R15	65	27	8	65	33	2	64	11	25	67	0	33	71	0	29	72	0	28	67	7	26	0	0,7	1,82	4,94																																										
	slurried div.	R10	54	27	19	66	28	6	67	8	25	61	2	37	42	3	55	54	2	44	46	18	36	0,04	0,76	2	1,81																																										
		slur.div.		60	27	13	65	31	4	66	9	25	64	1	35	57	1	42	63	1	36	57	12	31	0,02	0,73	1,91	3,38																																									
	basin plain	R5	59	30	11	64	30	6	67	12	21	46	18	36	63	23	14	63	6	31	64	4	32	0,23	0,65	2	2,75																																										
	basin plain	R12	52	34	14	58	34	8	60	5	35	47	3	50	60	3	37	66	1	33	56	16	28	0,03	0,87	1,53	2,32																																										
		basin		56	32	12	61	32	7	64	8	28	46	11	43	61	13	26	64	4	32	60	10	30	0,13	0,76	1,77	2,54																																									
	outer lobe	R3	67	25	8	72	24	4	73	6	21	69	0	31	77	0	23	65	0	35	59	9	32	0	0,79	2,69	2,09																																										
	outer lobe	R7	54	35	11	58	35	7	61	14	25	33	34	33	62	38	0	72	10	18	80	0	20	0,38	0,65	1,55	3,13																																										
		outer lobe		61	30	9	65	30	5	67	10	23	51	17	32	69	19	12	68	5	27	70	4	26	0,19	0,72	2,12	2,61																																									
		X		59	30	12	64	31	5	65	10	25	54	9	37	63	11	26	65	3	32	62	9	29	0,1	0,7	1,9	2,8																																									
	s.d.		6	4	4	5	4	2	5	4	5	14	14	7	12	16	19	7	4	9	11	7	6																																														
Pianello area	slurried div.	P26	56	39	5	60	39	1	59	17	24	77	0	23	89	0	11	76	0	24	73	3	24	0	0,59	1,44	8,54																																										
	fringe-basin	P18	62	26	12	72	26	2	71	11	18	82	0	18	100	0	0	64	0	36	64	0	36	0	0,62	2,4	2,09																																										
	fringe-basin	P22	62	30	8	68	30	2	67	9	24	81	0	19	78	0	22	71	0	29	69	3	28	0	0,73	2,03	3,11																																										
	fringe-basin	P21	50	39	11	60	39	1	57	15	28	87	0	13	84	0	16	75	0	25	72	3	25	0	0,65	1,29	3,35																																										
	fringe-basin	P2	45	43	12	54	43	3	51	17	32	76	0	24	91	0	9	90	0	10	88	3	9	0	0,65	1,04	3,51																																										
		fringe-basin		55	34	11	63	35	2	62	13	25	81	0	19	88	0	12	75	0	25	73	2	25	0	0,66	1,69	3,02																																									
	outer lobe	P5	36	49	15	47	49	4	43	12	45	74	0	26	91	0	9	69	0	31	67	2	31	0	0,78	0,73	3,48																																										
	outer lobe	P3	52	31	17	65	31	4	62	14	24	78	2	20	90	3	7	66	1	33	66	2	32	0,09	0,63	1,64	1,82																																										
	outer lobe	P23	27	54	19	35	54	11	34	23	43	37	8	55	56	9	35	68	4	28	61	14	25	0,09	0,65	0,51	2,8																																										
	outer lobe	P1	42	48	10	48	48	4	46	18	36	62	0	38	94	0	6	70	0	30	69	1	30	0	0,67	0,86	4,72																																										
		outer lobe		39	46	15	49	45	6	46	17	37	63	2	35	83	3	34	68	1	31	66	5	29	0,05	0,68	0,94	3,21																																									
		X		48	40	12	57	40	3	54	15	30	73	1	26	86	1	13	72	1	27	70	3	27	0	0,7	1,3	3,7																																									
		s.d.		12	10	4	12	10	3	12	4	9	15	3	13	13	3	10	8	1	7	8	4	8																																													

Clastic system	Petrological parameters and ratios						Lv%	Iv%	Q/F	F/L	P/F
	Qm	F	Lt	Lm	Lv	Ls					
<i>Poggio Belvedere sandstones (this study)</i>											
Maestà area	64 (12)	30 (10)	6 (2)	82 (8)	0	18 (8)	0	0	2,52	5,42	0,76
Renali area	59 (6)	30 (4)	12 (4)	63 (12)	11 (16)	26 (19)	14	11,25	1,93	2,84	0,74
Pianello area	48 (12)	40 (10)	12 (4)	86 (13)	1 (3)	13 (10)	4-2,5	2	1,33	3,71	0,66
<i>Macigno sandstones - northern Tuscany (Di Giulio, 1999)</i>											
Upper Macigno	54 (4)	29 (4)	17 (3)	84 (5)	11 (3)	5 (2)	1,9	1,8	...
Lower Macigno	55 (5)	26 (3)	19 (5)	70 (7)	21 (6)	9 (5)	2,2	1,5	...
<i>Macigno sandstones - Tuscany (Cornamusini, 2002)</i>											
Macigno Costiero petrofacies	57 (4)	19 (4)	24 (7)	66 (5)	19 (8)	15 (8)	≥ 13	19	3	0,792	0,3
Macigno Intermedio petrofacies	55 (4)	27 (2)	18 (5)	75 (7)	19 (7)	6 (5)	≥ 13	19	2,037	1,5	0,4
Macigno Appenninico petrofacies	59 (6)	25 (4)	16 (4)	82 (8)	11 (5)	7 (5)	< 13	11,5	2,36	1,563	0,45
<i>Macigno sandstones - Northern Umbria (Plesi et al., 2002)</i>											
Poggio Belvedere member	40–55	20–50	10–25	0,8–2,75	0,8–5	0,62
<i>Macigno sandstones - NW Tuscany (Bruni et al., 2007)</i>											
Upper Macigno	50 (6)	34 (8)	16 (4)	74 (9)	15 (7)	11 (8)	1,47	2,125	...
Lower Macigno	52 (3)	32 (4)	16 (2)	79 (8)	13 (6)	8 (5)	1,625	2	...
<i>Macigno sandstones - E Tuscany/W Umbria (Barsella et al., 2009)</i>											
Molin Nuovo member	49–74	28–42	9–26	42–59	30–38	6–20	1,2–2,6	1–4,7	...
Poggio Belvedere member	36–61	14–24	10–25	52–89	6–33	4–15	1,5–4,3	0,96–1,4	...
<i>Modern Calabria Arc sands</i>											
Granite sourced sands*	46	33	21	1,3	3,3	...
Metamorphic sourced sands*	55	24	21	2,4	1,4	...
Average*	51	28	21	88	0	12	0	0	1,821	1,333	...
Neto-Lipuda petrofacies**	36	46	18	86	0	14	0	0	0,783	2,556	0,7

Sample	Exp (I/S)	Exp (Chl/S)	Illite- mica	Kao	Chl	Σ Phy	Qtz	K-feld	Pl	Cal	Dol	
MA4	1	1	32		tr	22	56	22	1	12	7	0
MA1	1	1	29		tr	25	56	22	1	15	5	0
MA3	3	2	37		1	19	62	26	1	9	2	0
RA5	3	2	53		1	10	69	24	1	4	1	0
RA4	2	2	32		tr	12	48	22	2	19	9	0
RA3bis	1	1	32		tr	15	49	23	1	16	10	0
RA3	2	1	32		tr	14	49	23	1	15	11	0
RA1	1	1	35		tr	20	57	22	1	13	7	0
PA4	1	1	35		2	14	53	20	2	13	11	0
PA3A	1	1	33		2	13	50	25	2	17	5	0
PA2	2	1	48		1	13	65	24	2	7	2	tr
PA1	1	2	34		tr	16	53	24	2	15	5	tr

Sample	PA1	PA2	PA3A	PA4	RA1	RA3	RA3bis	RA4	RA5	MA1	MA3	MA4
<i>Oxides (wt%)</i>												
SiO2	53,29	53,17	53,05	48,04	50,56	49,66	49,76	50,64	52,57	49,44	54,30	49,65
TiO2	0,80	0,89	0,82	0,80	0,82	0,78	0,81	0,79	0,99	0,86	0,85	0,84
Al2O3	15,81	17,82	15,54	14,82	15,55	14,26	14,74	14,65	18,61	15,37	17,12	15,28
Fe2O3	7,03	5,86	7,06	7,38	7,88	7,53	7,55	7,38	5,74	8,59	7,11	7,90
MnO	0,07	0,08	0,08	0,08	0,08	0,08	0,08	0,09	0,04	0,08	0,06	0,09
MgO	6,75	5,73	6,28	6,58	6,42	5,81	6,17	6,25	6,37	9,69	6,58	8,11
CaO	3,33	1,65	3,81	7,03	4,71	6,86	6,16	5,97	1,34	3,33	1,72	4,67
Na2O	1,17	0,51	1,28	0,63	0,89	1,16	1,03	1,08	0,25	0,80	1,01	0,99
K2O	3,59	4,43	3,39	3,54	3,44	2,99	3,22	3,20	5,11	2,95	4,08	3,10
P2O5	0,11	0,08	0,12	0,08	0,08	0,11	0,10	0,11	0,05	0,08	0,10	0,09
LOI	7,33	9,35	7,70	11,00	9,31	9,93	9,91	9,41	8,57	8,71	6,66	9,04
Tot	99,28	99,57	99,12	99,98	99,74	99,17	99,51	99,56	99,64	99,90	99,58	99,76
<i>Trace elements (ppm)</i>												
V	154	178	164	175	164	141	160	152	180	176	164	168
Cu	36,88	33,23	42,14	34,08	45,21	17,76	50,39	59,46	35,8	48,16	32,8	45,19
Co	20,62	22,7	21,22	29,99	31,88	20,82	22,97	18,61	20,56	32,31	17,62	34,51
Cr	132	237	158	196	247	107	173	177	243	592	188	393
Ni	90,47	137,89	101,6	164,48	168,86	85,79	133,06	136,12	152,4	363,56	108,28	266,88
Zn	119,52	111,38	117,22	134,23	145,62	113,41	137,94	139,97	101,54	129,4	131,52	130,47
Sr	141	103	150	249	190	228	247	224	96	129	101	185
Ba	479	346	471	417	463	439	434	435	300	393	444	438
Rb	193	254	179	197	187	146	170	164	304	156	221	159
Y	32	31	28	31	28	21	34	35	40	29	30	30
Zr	177	183	168	128	138	147	152	157	197	156	172	155
Nb	17	20	18	18	17	16	17	15	23	16	19	16
La	43	60	39	36	29	16	35	39	69	40	57	43
Ce	84	134	69	91	75	64	96	97	144	86	109	84
Sn	10	9	6		9	14	5	7	9	6	6	7
<i>Ratios</i>												
ClA	66,48	68,05	66,89	68,44	64,80	68,72	67,10	67,62	66,47	70,43	68,54	70,20
ClA'	68,54	69,95	68,65	69,79	70,08	69,35	69,47	69,21	69,04	72,80	68,68	71,03
ICV	1,43	1,07	1,46	1,75	1,55	1,76	1,69	1,68	1,06	1,71	1,25	1,68
La+Ce/Cr	0,96	0,82	0,68	0,65	0,42	0,75	0,76	0,77	0,88	0,21	0,88	0,32
La+Ce/Co	6,16	8,55	5,09	4,23	3,26	3,84	5,70	7,31	10,36	3,90	9,42	3,68
La+Ce/Ni	1,40	1,41	1,06	0,77	0,62	0,93	0,98	1,00	1,40	0,35	1,53	0,48
Al/K	4,40	4,02	4,59	4,19	4,52	4,77	4,58	4,58	3,64	5,21	4,19	4,93
Rb/K	0,005	0,006	0,005	0,006	0,005	0,005	0,005	0,005	0,006	0,005	0,005	0,005
Cr/V	0,86	1,33	0,96	1,12	1,51	0,76	1,08	1,16	1,35	3,36	1,15	2,34
Y/Ni	0,35	0,22	0,28	0,19	0,17	0,24	0,26	0,26	0,26	0,08	0,28	0,11